Applications of Upper Limb Biomechanical Models in Spinal Cord Injury Patients

Angel Gil-Agudo[1], Antonio del Ama-Espinosa[1],
Ana de los Reyes-Guzmán[1], Alberto Bernal-Sahún[2] and Eduardo Rocón[3]
*[1]Biomechanics and Technical Aids Department. National Hospital for
Spinal Cord Injury, SESCAM.
[2]INDRA Sistemas S.A.
[3]Bioingeneering Group. CSIC,
Spain*

1. Introduction

Impaired upper limb function is one of the most common sequelae in central nervous system. In spinal cord injury (SCI) patients, upper limbs are affected in more than 50% of cases (Wyndaele and Wyndaele 2006). Upper limb strength is impaired to some extent in people who have suffered cervical SCI making it difficult for them to perform many activities of daily living (ADL) essential for their autonomy such as wheelchair manual propulsion, eating, drinking, and personal hygiene (Parker et al. 1986; Nakayama et al. 1994). In contrast with lower limbs, upper limbs have extensive functionally due to the mobility of numerous joints that can execute fine movements thanks to complex neuromuscular control. Lower limbs movements have been broadly analyzed in biomechanical studies specially regarding gait analysis. Gait analysis has evolved over the last decades as an important technique to assist in the clinical assessment of patients with mobility dysfunction. These techniques are useful for evaluation, treatment, and surgical planning; in addition, sequential assessments help to provide a functional outcome evaluation. Motion analysis offers an objective method for quantifying movement and is considered a gold standard for evaluating lower limb function during gait in different types of patients.

Therapeutic and surgical interventions to improve upper limb function primarily focus on muscle balance and joint position to maximize hand function; however, the methods for characterizing specific upper limb motion deficits and measuring the functional outcome are varied and mostly subjective. Upper limb function has traditionally been evaluated by different scales that only assess the quality of upper limb movement based on observational analysis, e.g. Fugl-Meyer Assessment, Frenchay Arm Test, Motor Assessment Scale, Action Research Arm Test, Box and Block Test, Nine Hole Peg Test (Wade 1992; Finch 2002). These outcome measures are reliable and sensitive for measuring gross changes in functional performance but have less sensitivity to smaller specific changes. These tools provide information concerning the quality of movement and a quantifiable score of performance,

yet they are lengthy, require the subjects to perform numerous tasks and are based on subjective and observational analysis.

A better understanding of upper limb movements requires more objective testing and accurate analysis of motion. Similarly to gait analysis, objective measurement elements and exact systems of movement analysis are necessary to be able to describe upper limb activities. Kinematic analysis is one such method. Kinematic describes movements of the body through space and time, including linear and angular displacements, velocities and accelerations, but without reference to the forces involved (van Anden et al. 2008). Three-dimensional motion capture systems have turned out to be a powerful tool for a quantitative assessment of movement in all degrees of freedom. Up to now, upper limb biomechanical analysis is not so often presented in the literature and in clinical practice, probably because motion analysis of the upper limb is more technically challenging. The models for lower extremity movements and gait analysis have been well established in biomechanical and clinical research and are now applied to the diagnosis and treatment planning of patients. However, the variety, complexity and range of upper limb movements is a challenge to assessment and interpretation of data and the clinical routines for 3-D analysis in upper limbs are not fully established (Murphy et al. 2006). The kinematic and kinetic equipments are ready to register, collect and analyze lower limb data from gait, but when considering upper limb movement it can be necessary to define and implement a biomechanical upper limb model that make more complex the analysis. On the other hand, gait analysis is a cyclic movement clearly defined and mainly in saggital plane but upper limb can perform a great variety of non-cyclic movements difficult to categorize in all planes. Finally, another point is the increased range and complexity of motion at the shoulder joint. As a result, few researchers have used motion analysis to characterize upper limb kinematics until recently, and there remains no generally accepted evaluation protocol.

Taking into account that most of population with SCI can not walk, upper limb biomechanical analysis of functional tasks becomes a very important issue. New applications of such studies are now continuously appearing. Data obtained from upper limb biomechanical analysis can be used not only for evaluation and treatment planning but also to give support to new research lines such as robot-assisted therapy or virtual reality applications in upper limb rehabilitation disorders (de los Reyes-Guzmán et al. 2010). In present chapter they are presented several different clinical applications of upper limb biomechanical studies in patients with SCI including biomechanical model description. First, it will be presented an upper limb model to study manual wheelchair propulsion in different levels of SCI; the second example is related to the biomechanical analysis of ADL such as drinking from a glass; it will also be described a clinical application of motor rehabilitation based on a virtual reality system with an upper limb biomechanical model developed and finally a model will be described to analyze tremor in upper limbs.

2. Clinical applications of upper limb biomechanical models in spinal cord injury patients

2.1 Manual wheelchair propulsion

Interest in the biomechanical analysis of manual wheelchair propulsion has increased as previous studies have reported an increasing age population of persons with SCI and a high incidence of upper extremity pathology. Although there is little research into the cause of repetitive strain injuries in manual wheelchair users there is abundance of reports

discussing the prevalence of this condition. The majority of the articles are surveys or interviews with the wheelchair users. Shoulder pain prevalence has been reported in 36% patients with paraplegia (Sie et al., 1992). It has been found 100% of the subjects more than 15 years out from SCI had shoulder pain as compared to 20% of those less than 15 years out from injury (Gellman et al. 1988). The most common neurologic cause of upper extremity pain in wheelchair users is carpal tunnel syndrome (CTS). The prevalence of CTS in this group is between 49% and 73% (Boninger et al. 1999).

Biomechanical analysis of wheelchair propulsion yields pertinent information to identify the factors that predispose to such injuries. The high prevalence of complaints is a clear indication that the mechanical load of wheelchair propulsion must be unfavorably high. One of the reasons for the high mechanical load can most likely be found in the fact that much muscular effort is needed for stabilization of the shoulder mechanism and especially for prevention of shoulder luxations. These extra muscular forces would then lead to overload of one or more of those muscles, but also to high compression forces in the gleno-humeral joint, which in turn might lead to damage to joint cartilage (van der Woude et al. 2001).

To date, most researchers have investigated many aspects of manual wheelchair propulsion predominantly in persons with paraplegia (Collinger et al. 2008). Only a few investigations focusing the biomechanical pattern of manual wheelchair propulsion have taken into account persons with tetraplegia (Newman et al. 1996; Newman et al. 1999; Dallmeijer et al. 1994; Dallmeijer et al. 1998; Kulig et al. 2001; van Drongelen et al. 2005) although it has been found a greater proportion of individuals with tetraplegia experienced shoulder pain as compared with paraplegic subjects (Curtis et al., 1999). Specific topics such as hand-rim force application (Dallmeijer et al. 1998) or shoulder joint kinetics (Kulig et al., 2001) and global aspects such as wheelchair propulsion temporal characteristics (Newman et al., 1996) or upper-limb kinematics (Newman et al. 1999) have been studied in wheelchair users with different levels of SCI including those with cervical level injuries. These studies suggested that the subject´s level of SCI could influence the biomechanics of wheelchair propulsion. But little information has been reported on global upper limb kinetics pattern. Only one study was found of the upper extremity kinetics during wheelchair propulsion in a group with upper limb impairment (Finley et al. 2004). In another previous report, two populations of patients with SCI were compared (Bednarczyk and Sanderson 1994). With the help of kinematic analysis, these authors found that children propelled their wheelchair in the same manner as adults. Information regarding the kinetics approach of manual wheelchair propulsion in population with paraplegia and tetraplegia will increase the overall knowledge base about performance of the task in each group of wheelchair users. It may provide insight into mechanisms of secondary pathologies and criteria for specific ergonomic wheelchair design for each group of users.

The ability of an individual to push a wheelchair efficiently and without injury is related to the way in which the users apply force to the pushrim during propulsion. A number of factors influence the interaction between user and wheelchair, including level of SCI, design of the wheelchair, fit between user and chair, stroke mechanics, user fitness levels and history of upper-extremity injury. Understanding how forces generated by the individual are applied to the pushrim will provide insight into how these forces are related to optimizing efficiency, improving performance, identifying mechanisms of injuries, developing injury prevention techniques and implementing changes in wheelchair design (Cooper 1995). So, first of all, it is necessary to measure pushrim forces and then try to calculate joint kinetic data.

The complexity of developing a system for measuring pushrim forces is evident. A number of researchers have attempted to develop a force-sensing system with varying degrees of success. The wheelchair kinetic data reported in the literature can be divided into three catergories: (1) static force measurements using, for instance, a system of springs to restrain a pushrim (Brauer and Hertig 1981), (2) external devices for measuring forces and torques like a force plate to measure the force generated during the initiation of wheelchair propulsion for the grab and start technique (Tupling et al. 1986) or a wheelchair with a gear attached to the hub connected by a chain and gear to an isokinectic dynamometer (Samuelson et al. 1989) and (3) measurement of force components at the pushrim (indirectly or directly) using a system based upon a special wheel with a slotted disk mounted to the hub with three beams instrumented with strain gauges like SmartWheel system. This system allows measurement of puhsrim forces in the plane of the wheel and the turning moment about the hub axis when mounted on everyday chairs. (Cooper 1995).

To get an impression of the mechanical load, joint kinetic data and the underlying mechanisms, a biomechanical model is a prerequisite. For calculation of the extra forces that would be necessary to stabilize the shoulder, a model would be required that is not only able to calculate net joint torque, but also to calculate individual muscle forces (van der Woude et al. 2001)

In biomechanics, the inverse-dynamic modeling approach is often used. The inverse-dynamic modeling approach takes its starting point, contrary to the direct-dynamic approach, in the resulting movement and external forces. This approach has been widely used in robotics to estimate robot joint torque and forces needed to move the robot. The robot is modelled as an articulated chain and, starting from the last segment, joint forces and moments are estimated by using the Newton's second and third laws (Figure 1). This procedure can be used to estimate net joint torques and forces in the human members, but introducing some modifications into the equations. Newton's second law for linear and angular movement is expressed by:

$$\sum \mathbf{F}_i = m_i \cdot \mathbf{a}_i \quad \sum \mathbf{M}_i = \frac{d\mathbf{H}_i}{dt}$$

If those equations are developed for an arbitrary segment of the upper extremity (Figure 1), we get the following expressions

$$\sum \mathbf{F}_{i,p} = m_i \cdot \mathbf{a}_i + m_i \cdot g\mathbf{j} + \sum \mathbf{F}_{i,d}$$

$$\sum \mathbf{M}_{i,p} = \left([I]_i \cdot \frac{d\boldsymbol{\omega}_i}{dt} + \boldsymbol{\omega}_i \times \left([I]_i \times \boldsymbol{\omega}_i \right) \right) - \sum \mathbf{M}_{i,d} - \left(\mathbf{c}_i \times m_i \cdot g\mathbf{j} \right) - \sum \left(\mathbf{d}_i \times \mathbf{F}_{i,d} \right)$$

Those equations give the proximal net force and torque from the distal net force and torque, as well as the movement and the inertial characteristics of the segment. Therefore, the input of the inverse-dynamic model comprises anthropometry, the movements and the torques and forces resulting from the interaction of the segments with the environment. This implies, of course, that they have to be measured.
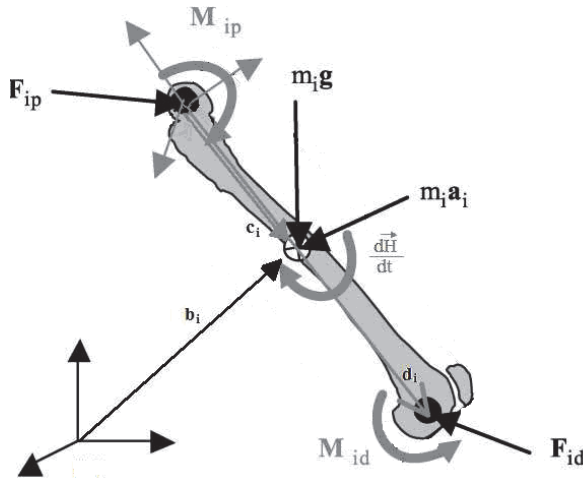
Fig. 1. Arbitrary body segment.

The anthropometric model represents the inertial and mass characteristics of the segments. The anthropometric model of the upper limb presented in this chapter follows the mathematical model of the human segments developed previously (Hannavan 1966). This model assumes the human limbs as rigid solids which shape is assumed to be revolute segments. Then, this model is corrected with Clausser's density coefficients (Clauser et al. 1969). As result, center of mass position and magnitude, segment geometry and inertial characteristics are easily linked to the anthropometric measures over the subject.

Kinematic model refers to the mathematical manipulation of the movement data acquired by the kinematics equipment (usually marker positions but there is a growing interest in using inertial measurement units) in order to match the angular velocity and acceleration of the above equations. Also, the kinematic model is used to report segment and joint kinematic. There are several mathematical approaches to solve and represent the relative kinematic of a segments chain, i.e. the helical axis, quaternion or the Euler angles are among the most used in the literature. However, in clinics the limb movements are usually described with respect to the anatomical planes of the body, projecting the segment or joint movement into the saggital, coronal and frontal plane of the body or the segment. Therefore, the use of Euler angles has been taken as the basis to solve the segment kinematics in the model developed to analyze manual wheelchair propulsion. However, one of the disadvantages of Euler angles with respect to other methods is that Euler angles are dependent on the order of rotations chosen to solve the 3D segment rotation, so care must be taken in order to define the rotation sequence to accomplish main objectives: first is to avoid indeterminations while calculating the Euler angles, whereas the second objective is to guarantee that the results can be easily compared with the literature, which only can be guaranteed if the same rotation sequence is used. In this respect, the kinematic model of the upper limb presented in this chapter has been developed taking into account the International Society of Biomechanics recommendations to define both the local reference systems for the upper limb segments as well as the order of rotations (Wu et al , 2005). Kinematic data can be measured with sophisticated high-speed automatic systems based upon active or passive markers technology, in which the absolute position of the markers is

measured. In some type of movements a two-dimensional system usually suffices because it can be assumed that movements in other planes are small and also of lesser importance. For wheelchair propulsion this obviously is not the case as movements do not occur in one plane. There is a growing interest on the use of the inertial measurement technology, which gives the absolute pose of the body (assumed rigid) in which the unit is attached.

Both anthropometric and kinematic model are joined in the dynamic model given by the above equations to form the general dynamic model of a segment (Fig. 2). As mentioned above, net proximal joint moment and forces are solved with respect to the distal ones, so a recursive procedure can be easily implemented to solve the whole segment dynamics. This recursive algorithm begins at the contact point of the segment with the environment, the handrim in the case of manual wheelchair propulsion, where it is necessary to record the externally applied forces and moments. These forces can only be measured with highly specialized equipment such as wheelchair simulator (Niesing et al. 1990) or instrumented wheels like Smart-Wheels (Cooper et al. 1997) or Opti-Push (Max-Mobility, 5425 Mount View Parkway, Antioch, TN).
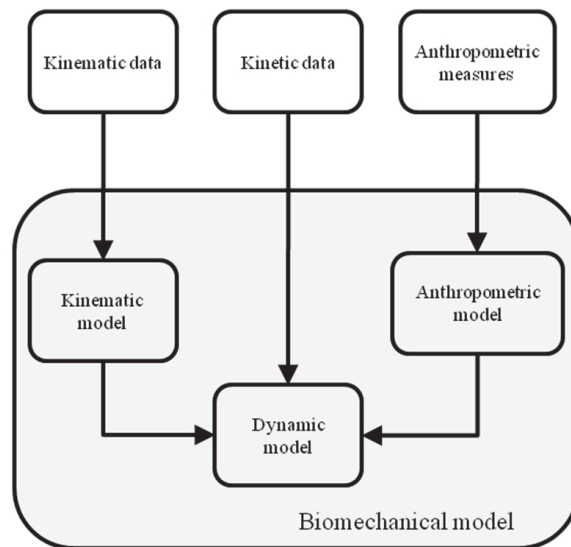

Fig. 2. Biomechanical model composition.

Most inverse-dynamic models are capable of calculating the net joint torque and power (Cooper et al. 1996; Cooper et al. 1997; Rodgers and Tummarakota 1998; Rodgers et al. 2000; Boninger et al. 1997, Boninger et al. 1999). Net torque values give a good indication of the net muscular forces that are needed around a joint. However, these torques are net values, which implies that they are the sum of all muscle force around that joint. Net torque values are thus likely to be underestimations of the actual muscle forces. If, for instance, two antagonists produce the same force against the same torque arm, the resulting force will be zero, while the sum of muscle forces is not. In the shoulder, it is likely that, because of the need for sufficient joint stability, antagonists will be active at the same time. In analyses of muscle function in the shoulder, a biomechanical model will therefore be needed that estimates the contribution of

muscles to net torques and resulting movements. A biomechanical model has been developed which includes muscles of the arm and shoulder. This model can now also be applied to manual wheelchair propulsion (van der Helm and Veeger 1999).

In a previous report, the influence has been analyzed of different levels of SCI in upper limb kinetics during wheelchair propulsion taking into account a biomechanical model using inverse-dynamic model (Gil-Agudo et al. 2000). Therefore, the purpose was to compare the forces and moments at shoulder, elbow and wrist during wheelchair manual propulsion of persons with four different levels of SCI (two tetraplegic and two paraplegic) on a treadmill. It was intended that the findings from this study will provide a baseline for future comparisons with data from wheelchair users with any upper limb impairment.

Fifty-one persons were enrolled in this study. The inclusion criteria required that subjects have a SCI with neurological level between C6 and L3, with severity classified by American Spinal Injury Association as ASIA A or B (Maynard et al., 1997), age over 18 and under 65 years, duration of the injury of at least of 6 months, no history of shoulder pain conditions and no regular participation in sports activities. Subjects were categorized into four groups according to the neurological level of their lesion: C6 tetraplegia (G1, n=12), C7 tetraplegia (G2, n= 8), paraplegia between D1-D10, also known as "high paraplegia" (G3, n=17) and paraplegia between D11 and L3, or "low paraplegia" (G4, n=14). A standard adjustable wheelchair, the Action3 Invacare (Invacare Corp, Elyria OH, USA), was properly fitted to each subject and placed on a treadmill (Bonte Zwolle B.V., BO Systems, Netherlands). Power output was determined in the form of a drag test in which the drag force of the wheelchair-user system was measured (van de Woude et al. 1986) with a force transducer (Revere ALC 0,5. Vishay Revere Transducers BV. Breda, The Netherlands). After a two-minute adaptation period, participants propelled the wheelchair at 3 km/h during one minute. We used a digital slope meter (Solatronic EN 17, Fisco Tools Limited. Brook Road, Rayleigh, Essex, UK) to verify that the treadmill surface remained parallel to the floor at all times. Propulsion trials on the treadmill were conducted with a safety system. A spotter at the front of the treadmill controlled the safety tether.

The biomechanical model is focused on the shoulder and did not consider the movements of the scapula, clavicle and thoracic spine. The net forces and moments were transformed to the local coordinate system of the proximal segment of the shoulder joint, i.e., the trunk. All shoulder joint net forces and moments were referenced to the trunk local coordinate system (Cooper et al. 1999; Mercer et al. 2006). Segment kinematics was recorded from right upper limb, where reflective markers were positioned following ISB recommendations (Wu et al., 2005) to define local reference systems on the hand, forearm and arm (Figure 3). Trunk local reference system was modified and defined using markers placed on the seventh cervical vertebra (C7) and on the right (ACRR) and left (ACRL) acromio-clavicular joints (Figure 3). The axes of this reference system were calculated as follows:

The Z-axis (+extension/-flexion) was formed with the right and left acromio-clavicular markers:

$$\vec{z}_{trunk} = \frac{\vec{ACR_R} - \vec{ACR_L}}{\left\| \vec{ACR_R} - \vec{ACR_L} \right\|}$$

The y-axis (+rotation toward the left/-rotation toward the right) was defined as the cross product of the z-axis and the vector formed by the markers on the seventh cervical vertebra and left acromio-clavicular joint:

$$\vec{y}_{trunk} = \frac{\left(C7 - \vec{ACR_L} \right) \times \vec{z}_{trunk}}{\left\| \left(C7 - \vec{ACR_L} \right) \times \vec{z}_{trunk} \right\|}$$

The x-axis (+ right tilt/- left tilt) was defined as the cross product of the y-axis and the z-axis:

$$\vec{x}_{trunk} = \frac{\vec{y}_{trunk} \times \vec{z}_{trunk}}{\left\| \vec{y}_{trunk} \times \vec{z}_{trunk} \right\|}$$

Finally, to ensure the orthogonality of the reference system of the trunk, the definitive z-axis was calculated as the cross product of the x and y vectors:

$$\vec{z}_{trunk} = \frac{\vec{x}_{trunk} \times \vec{y}_{trunk}}{\left\| \vec{x}_{trunk} \times \vec{y}_{trunk} \right\|}$$

Photogrametric data was collected at 50 Hz with four camcorders (Kinescan-IBV, Instituto de Biomecánica de Valencia, Valencia, Spain). Once digitalized, spatial marker coordinates were smoothed out using a procedure of mobile means. The kinetic data were collected by replacing the wheels of the chair by two SMART[Wheels] (Three Rivers Holdings, LLC, Mesa, AZ, USA). It was assumed that the force was applied on the third metacarpal as the point of hand contact (Cooper et al., 1997). However, in the case of the tetraplegic subjects, the point of contact with the pushrim was assumed to be the proximal part of the palmar face of the hand, due to the weaker grip of these subjects. A synchronization pulse from the Kinescan-IBV was used to trigger the start of kinetic and kinematic collection. Kinetic data were recorded at a frequency of 240 Hz and filtered using a Butterworth, fourth-order, low-pass filter with a cutoff frequency of 20Hz and a zero phase lag. Spatial marker coordinates were interpolated by cubic spline to synchronize with the kinetic data. All subjects were right-hand dominant. The data recorded with the right wheel were used for the kinetic analysis. The left wheel also was replaced to balance the inertial characteristics of both axes and thus ensure symmetrical propulsion.

Once solved the dynamic model with anthropometric, kinematic and kinetic data from the trials, joint net forces and moments were transformed to the local coordinate system of the proximal segment of the joint. The forces reported constituted the reaction forces on the joint, expressed on the proximal reference system of the joint. Moments were reported as the action moments and also expressed on the proximal reference system of the joint.

In this comprehensive analysis of the upper limb kinetics during manual wheelchair propulsion of persons with levels of SCI from C6 tetraplegia to low paraplegia, our initial hypothesis was confirmed: differences were found between persons with paraplegia and tetraplegia. Most of the

differences were found in vertical axe and were related to wrist kinetics. They could be attributed to absence of intrinsic hand musculature in persons with tetraplegia.

Fig. 3. Reflective marker placement.

The presence or absence of abdominal musculature in the two paraplegic groups did not alter any of the kinetics recorded in the upper limb, as previously reported in kinematic upper limb analysis (Newman et al. 1999). Two different manual wheelchair propulsion patterns of upper limb kinetics in persons with upper limb impairment have been proposed. In an earlier study, individuals with altered upper limb strength generated increased medial forces on the pushrim to provide the necessary friction to maintain grip (Dalmeijer et al. 1998). The other wheelchair propulsion pattern described involves the reduction of joint excursion and contact time with the pushrim, which constrains the user-wheelchair interface and may allow a larger percentage of tangential force to be applied (Finley et al. 2004). However, medial forces on the pushrim were not increased and hand contact time was not reduced in our current study.

The most noteworthy findings in both tetraplegic groups were an increase on upward joint forces in the shoulder, elbow and wrist and an increased adduction moment in the shoulder. Comparisons between studies are often difficult because of different testing procedures, units of measurement, equipment employed and characteristics of the sample studied (Finley et al. 2004). In this study, propulsion analysis was carried out using a wheelchair placed on a treadmill, which some authors have characterized as the ideal mechanical situation (Richter et al. 2007). Other investigators have used dynamometers (Kulig et al. 1998; Newman et al. 1999; DiGiovine et al. 2001) or ergometers (Niesing et al. 1990). Another differential aspect between studies is the testing velocity. Most studies report that net forces and moments depend strongly on the propulsion speed (Koontz et al. 2002; Veeger et al. 2002; van Drongelen et al. 2005; Collinger et al. 2008). A uniform velocity (3 km/h) for all subjects was chosen in this study to optimize test performance in

the tetraplegic group and to provide a control within the testing protocol. This allowed group differences to be determined (Finley et al., 2004) and ensured a submaximal exercise level for all subjects (van Drongelen et al., 2005). The characteristics of our four SCI groups were the same as in studies by other investigators (Kulig et al. 2001; Newman et al. 1996; Newman et al. 1999).

Due to their limited physical capacity, subjects with tetraplegia applied force to the pushrim ineffectively. They propelled the wheelchair with an increased push/recovery time, but achieved less distance with each stroke. The predominance of the adductor moments of the shoulder forces during the push phase is due to similar mechanisms as the increased lateromedial forces on the pushrim reported in other studies (Djalmeijer et al. 1998). Both mechanisms allow people incapable of actively extending the elbow and with impaired hand strength to bring the upper limb closer to the pushrim.

The upper limb joint kinetics pattern identified in the present study provides some insight into why people with SCI have a high prevalence of shoulder and wrist pain (Sie et al. 1992; Gellman et al. 1988; Subbarao et al. 1995), especially in the case of tetraplegia (Curtis et al. 1999). The predominant force in people with tetraplegia is applied to the pushrim abruptly and downward on the vertical axis. This force of action on contact with the pushrim elicits an opposite force of reaction that is transmitted to all the upper limb joints, so that there is a clear predominance of upward vertical forces during the push phase in every joint. This situation predisposes to the compression of structures like the median nerve in the carpal tunnel or the rotator cuff in the subacromial space due to elevation of the humeral head. In an earlier study no increase in the joint compression forces was found in people with upper limb impairment, probably because the propulsion conditions were not uniform for all the groups (Finley et al. 2004). The net joint moments of the glenohumeral joint correlate closely with the glenohumeral joint compression forces (Praagman et al. 2000, Mercer et al. 2006) and pushrim forces have been related to carpal tunnel syndrome (Gellman et al. 1998; Boninger et al. 1999).

Most kinetic differences between people with tetraplegia and paraplegia can be attributed to the point of force application of the hand on the pushrim, which influences the calculation of hand torque (Linden et al. 1996). In the case of people with paraplegia, the point of application of force is located at the head of the third metacarpal. However, people with tetraplegia lack full hand muscle function and it is more difficult for them to grasp the pushrim. Consequently, the point of application of the force is shifted to the proximal part of the hand. This involves a change in the model with backward displacement of the point of application of force, which originates relevant differences in the moments of force on the carpus. In the tetraplegic groups, the joint moments remained practically constant throughout the cycle. The value of the joint moments depends on inertia and muscular action. Since the muscular action is practically nonexistent in people with tetraplegia, the final result depends on inertia alone, which in turn depends mainly on weight, making it an almost constant value.

2.2 Biomechanical analysis of activities of daily living

Upper limb functionality is fundamental for the execution of basic (ADL) like drinking, eating and personal hygiene. Upper limb strength is impaired to some extent in people who have suffered cervical SCI. They may require technical assistance. Therefore, these patients

experience sharp limitations in their level of activity and participation in the social setting, as people who have suffered another central nervous system injury, such as stroke (Broeks et al. 1999).

Until now, upper limb function in ADLs has been evaluated mainly using a serie of functional scales. These tools are sensitive to gross functional changes, but less sensitive in measuring small and more specific changes (Murphy et al. 2006). Moreover, the use of these scales is not exempt from a degree of subjectivity.

Biomechanical analysis and, specifically, kinematic analysis techniques are interesting tools for obtaining objective data. Complex systems of kinematic analysis allow movement analysis in three dimensions. In order to analyze the upper limb movement it is necessary to define and to develop the biomechanical model based on the activity to be analyzed.

Kinematic studies have considered upper limb in which reaching/grasping movements on a horizontal plane as a free movement without arm support (van Anden et al. 2008) and with arm support (McCrea et al. 2002; Dwan and McIntosh 2006) have been analyzed. However, the analysis of purpose-oriented movements must be proposed because the musculoskeletal system has potentially a larger number of ways to achieve the motor task, permitting the organism to adapt to different environmental conditions. So, the musculoskeletal system takes advantage of this feature of the motor apparatus by selecting a desired trajectory and an interjoint coordination among many possible strategies to make goal-oriented movements (Roby-Brami et al. 2003). Studies have been published on kinetic analysis of the shoulder and elbow in healthy subjects performing a set of ADLs (Murray and Johnson 2004; Murgia et al. 2004) and on complete kinematic analysis of the upper limb during the movement of drinking from a glass (Murphy et al. 2006).

It has been confirmed that movement characteristics can vary depending on the objective to be completed. For example, upper limb kinematics is not the same in pointing to an object as when a grasping function is added (Dwan and McIntosh 2006; Safaee-Rad et al. 1990). Several studies have been published recently on the three-dimensional analysis of ADLs in healthy subjects (Murphy et al. 2006; van Anden et al. 2008; Petuskey et al. 2007). Similar studies have been made in patients with different neurological conditions (Mosqueda et al. 2004; Fitoussi et al. 2006). Although there have been few reports in patients with SCI, the results of the kinematics of grasping and the movements of pointing toward an object in patients with C6 tetraplegia have been described (Laffont et al. 2000). However, recently, it has been reported a methodology to analyze the kinematic data of the upper limb when performing a functional activity like drinking from a glass in patients with different levels of cervical SCI (de los Reyes-Guzmán et al. 2010) which is going to be developed here.

Twenty-four subjects divided into three groups were included in this study: a control group (CG), subjects with metameric level C6 tetraplegia (C6 group) and subjects with metameric level C7 tetraplegia (C7 group). Each group contained 8 subjects. All subjects were right-handed. In the case of subjects with C6 and C7 tetraplegia, the etiology of injury was trauma in every case. The patients screened had to fulfill the following criteria to be included in the study: age 16 to 65 years, injury of at least 6 months' duration and level of injury C6 or C7 classified according to the American Spinal Injury Association (ASIA) scale into grades A or B (Maynard et al. 1997). Patients who presented any vertebral deformity, joint restriction, surgery on any of the upper limbs, balance disorders, dysmetria due to associated neurologic disorders, visual acuity defects, cognitive deficit, or head injury associated with the SCI were excluded. The subjects were classified into C6 or C7 tetraplegia by a physical examination.

Three-dimensional movement capture was recorded with CodaMotion equipment (Charnwood Dynamics, Ltd, UK). This equipment has active markers that emit infrared light, which was recorded by two scanning units in this study. The marker images are displayed on a computer screen and projected as X, Y, and Z coordinate values.

One of the cameras was placed in front of the table, slightly to one side with respect to midline and contralateral to the study side of the subject. The other camera positioned laterally in the same side of experimentation (Figure 4). The system was calibrated by placing three active markers on the floor to serve as the laboratory reference system. The coordinate system was defined with the X-axis directed forward (anterior), the Y-axis upward (superior) and the Z-axis to the side (lateral) (Wu et al. 2005). The location of the cameras and markers was validated with a person sitting in the measurement area to ensure that the markers were recorded at least by one of the cameras throughout the drinking activity.
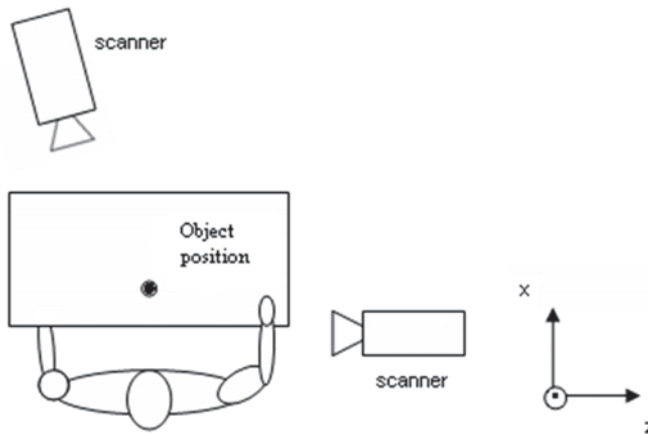
Fig. 4. View from above of the set-up for the activity of drinking from a glass. The XYZ coordinate system is visible. The subject has the arm at the starting point.

Eighteen markers were used. Following the recommendations of earlier studies, the body segments were defined by placing 8 markers on the superficial bony prominences of the right upper limb, which were easily positioned in the different analyses (Cirstea and Levin 2000; Michaelsen et al. 2001; Murphy et al. 2006; Dwan and McIntosh 2006). These markers were placed on the head of the third metacarpal, radial and ulnar styloid processes of the wrist, lateral and medial epicondyles of the elbow, right and left acromion and right iliac crest. The biomechanical model of upper limb movement was completed with another 10 markers mounted on rigid pieces that were placed on each body segment. These pieces were used with the aim of minimizing any error created by possible marker displacement on the skin. These pieces had to be light, comfortable for the subject to wear, and had to be fixed onto points where the least amount of movement was possible (Fitoussi et al. 2006). Four markers were placed on the chest, three mounted on a support and one directly on the skin; three markers mounted on a support placed on the arm, and the last three markers mounted on a support placed on the forearm (Figure 5). The final position of the last 10 markers and the position of the cameras was the position that yielded the best marker visibility to the scanning cameras during the movement of drinking from a glass and the best measurement results in the processed recordings.
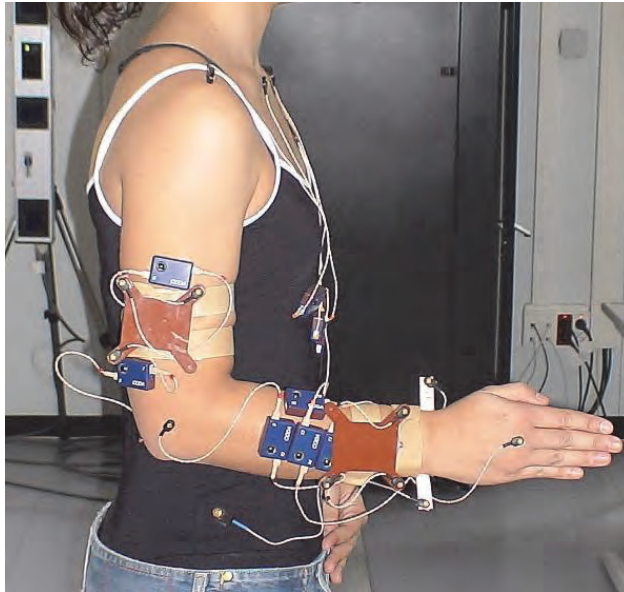
Fig. 5. Actual markers position on the subject. Figure show a sagittal plane view (X-Y).

All subjects were right-handed and performed the drinking task with the right arm. Subjects with C6 or C7 tetraplegia sat in their own wheelchairs and the control subjects sat in a conventional wheelchair, Action3 Invacare (Invacare Corp, Elyria OH, USA) with a configuration similar to that of the wheelchair of the subjects with tetraplegia. The chair was placed before a table measuring 120x60x72 cm. In every case, the subject-to-table distance was 18-20 cm and the angle between the seat and back was 90-100º. The starting position (position of calibration) for all the subjects was defined as a position in which the subject's trunk rested firmly against the back of the chair. All subjects put their feet on the footrests with a foot-leg angle of 90º. The right upper arm was placed against the trunk and the elbow was flexed 90º flexion and in a neutral pronation-supination, i.e., with the palm of the hand perpendicular to the table surface and facing inward (medial). The ulnar side of the wrist rested close to the surface of the table. In every case, the sitting and table heights could be adapted with the aim of obtaining the same starting position for all the subjects. The subject rested the left hand on the lap. A hard plastic glass measuring 6.5 cm in diameter by 17.5 cm high was used. It was filled with 1 dl of water and placed 18 cm from the edge of the table where the subject was seated, in the area marked on the table (Figure 4).

Each subject received an explanation about how to perform the drinking task, which consisted of reaching out for the glass from the starting position and grasping it, raising the glass to the mouth, drinking, lowering the glass to the pickup point, and returning the hand to the starting position. All the subjects practiced the activity twice to find a comfortable sitting position before the movement exercise was recorded. This test confirmed that the subjects could carry out the activity. Once this phase was completed, a static calibration recording was made. Using the static calibration recording, it was checked that each marker was visible at least by one of the scanning cameras at all times. Movement recordings were made as the subject executed the drinking task at a comfortable, self-selected speed. Before a

recording was accepted as validated, it was checked it to ensure that the markers were visible at all times. Five valid recordings of each subject were obtained for analysis and processing.

The consistency and repeatability of the test protocol were assessed by conducting a test-retest sequence with four randomly selected control subjects. Test-retest involved recording the action of the drinking task and then removing the markers. The entire procedure was repeated fifteen minutes later.

The recordings were processed with Visual 3D software (C-Motion, Inc., USA), which involved using a signal processing program to obtain signals of the movement of different joints at a sampling frequency of 200 Hz, the maximum allowed for the 18 markers used with the two scanning units. Signals were filtered using a low-pass Butterworth filter with a cutoff frequency of 1.5Hz. The three best recordings were selected from the five recordings made on the basis of best marker visibility in each recording. The mean of these three recordings yielded the final measurement value for each subject. The human arm was modelled for three-dimensional kinematic analysis in three segments, the arm, forearm and hand, which were considered as rigid solids (Biryukova et al. 2000). A local coordinate system was defined for each segment following the recommendations of the International Society of Biomechanics (Wu et al. 2005). In the arm, the origin of the reference system was at the center of the glenohumeral joint, 2 cm below the acromion. Also, the Y-axis corresponded to the line that joined the midpoint between the lateral and medial epicondyles and the center of the glenohumeral joint in proximal direction and the Z-axis was the mediolateral axis pointing to the right. In the forearm, the origin was at the midpoint between both epicondyles of the elbow, the Y-axis was formed by the line that joined the midpoint between the radial and ulnar styloid processes with the midpoint between the lateral and medial epicondyles proximally and the Z-axis was the line that joined both epicondyles in the lateral direction. In the hand, the origin was at the midpoint between radial and ulnar styloid of the wrist, the Y-axis was the line joining the head of the third metacarpal with the midpoint between the radial and ulnar styloid processes proximally and the Z-axis joined both styloid processes laterally. We obtained trunk movement with respect to the laboratory coordinate system, arm movement with respect to the trunk, forearm movement with respect to the arm, and hand movement with respect to the forearm using Euler angle notation and a sequence of ZXY rotations of the trunk, arm and hand, and ZYX rotations of the forearm.

In each recording, a complete cycle of the drinking task was identified. The beginning of the cycle was the onset of displacement of the marker on the head of the third metacarpal and the end of the cycle was the return of the marker to the starting point after completing the drinking task. As it happens with other cyclical movements, such as walking, several phases were established in the drinking task to facilitate task analysis. Phases and events delimiting the phases have been previously described: reaching, forward transport, drinking, back transport and return (Murphy et al. 2006).

Once the recordings were made and analyzed, the results were described in terms of analysis of the following variables:

- Movement times: the duration of each phase and the complete cycle.
- Peak velocities: the velocities were obtained by calculating the linear velocity with which the hand moves in the phases of the cycle of reaching, forward transport, back transport and return to start position.

- Joint angles: flexion-extension and lateral inclination of the trunk; flexion-extension, abduction-adduction and external-internal rotation of the shoulder joint; flexion-extension and pronation-supination of the elbow joint; and dorsal-palmar flexion of the wrist. For each joint angle, we calculated the maximum, minimum, range of motion (ROM) and moment in the complete drinking cycle in which these values were reached.
- Coordination between the shoulder and elbow joints, particularly between the shoulder flexion angle and the elbow flexion angle, in the reaching phase.

In order to compare the three groups analyzed, the duration of the cycles was adjusted for time and expressed as percentages. Consequently, data were expressed in relation to the percentage of the drinking task cycle that had lapsed (0-100% of the drinking task cycle) when the movement was recorded.

The goal of this study was to analyze the three-dimensional kinematic differences between two groups of people with tetraplegia and a control group during the ADL of drinking from a glass. The most relevant findings of this study suggest that subjects with C6 tetraplegia perform the drinking task at a slower velocity and with more prolonged phases. The greatest differences between the two tetraplegia groups and controls were in the wrist.

However, more functional movements should be studied. Previous studies of upper limb kinematics have been made of control subjects performing ADLs such as feeding, grooming and drinking (Cooper et al. 1993; Magermans et al. 2005; Murphy et al. 2006). These movements are complex tasks in terms of kinematics because they consist of several discrete movements.

Much of the methodology reported here followed the recommendations of a previous one of healthy subjects in which five sequential phases of drinking task were identified (Murphy et al. 2006). However, the current experience has resolved previous limitations and provides a full and detailed three-dimensional kinematic analysis of the drinking task in control subjects and two groups of patients with tetraplegia, analyzing the shoulder, elbow and wrist at all possible joint angles except for lateral wrist inclination.

Using the upper limb model developed, we were able to estimate the location of the center of the joints involved, which made it possible to measure all the joint angles described. Likewise, the use of markers mounted on rigid pieces to position some of the markers helped to reduce tissue artifacts. These artifacts appear with limb displacement when markers are placed on the skin surface.

The duration of the drinking activity was longer in subjects with C6 tetraplegia compared to controls and the duration of the reaching phase was longer in subjects with C6 and C7 tetraplegia. As mentioned, the reaching phase includes grasping. In order to grasp, both groups of patients with tetraplegia developed a compensatory strategy called "tenodesis," in which these patients extend the wrist to close the fingers passively. This pattern suggests that in subjects with tetraplegia reaching and grasping are executed sequentially compared to controls, who prepare for grasping during the reaching phase (Jaennerod 1984).

The absence of triceps brachialis muscle activity in subjects with C6 tetraplegia slows the velocity of the forward transport and back transport phases, in which this muscle controls the eccentric or concentric displacement of the elbow in flexion-extension. As in an earlier study, the peak velocity of the reaching phase was similar in patients with tetraplegia and controls (Laffont et al. 2000). Another factor that could condition the velocity of movements is performing the movement with a load. Upper limbs weakness becomes more evident

when raising an object with a certain weight. In the absence of any additional load, peak velocity in the reaching phase is reached earlier in groups of patients with tetraplegia. However, in the forward transport phase, the glass of water is raised to the mouth and the peak velocity is notably faster in controls. It is difficult to compare the velocities obtained in other pathologies because they have not been studied using the phases defined in our study (Rönnqvist and Rösbled 2007).

In a reaching movement, as shoulder flexion increases, elbow extension also increases. So it was interesting to know the index of coordination between both movements (de los Reyes-Guzmán et al. 2010). This coordination is shown in Figure 6 and the trajectory is continuous describing an almost linear relation between shoulder and elbow flexion movements. The result was that, as in healthy subjects, but in contrast with subjects who have experienced stroke and have a hemiparetic arm, there was a strong coordination between shoulder and elbow joint excursion in the reaching phase, indicating good interjoint coordination in C6 and C7 tetraplegic people (Levin 1996) (Figure 6).
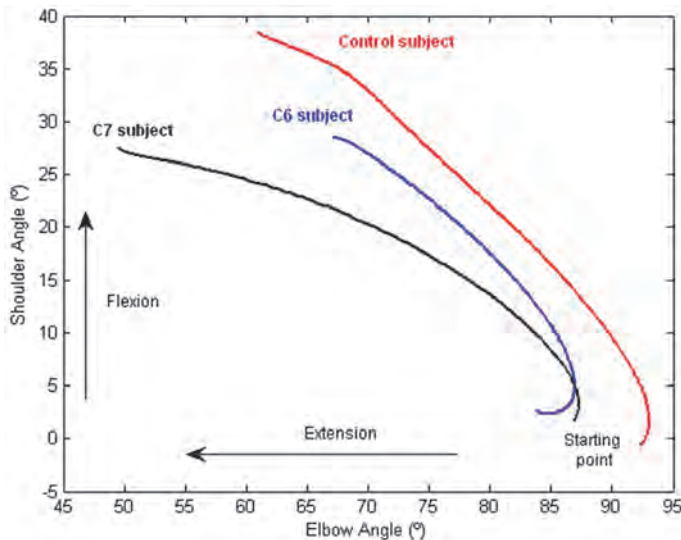

Fig. 6. Shoulder-elbow joint coordination in the reaching phase for one randomly selected subject in the control group (red), C6 group (blue) and C7 group (black).

The wrist was the joint with the most relevant differences between the three groups. Wrist palmar flexion angles were greater in both groups of subjects with tetraplegia and the maximum wrist palmar flexion in both cases was observed in the back transport phase, probably because no eccentric resistance is offered by wrist extensor muscles as the glass is lowered from the mouth to the table; passive wrist palmar flexion occurred in both tetraplegia groups. The minimum wrist palmar flexion angle was found in subjects with C6 or C7 tetraplegia in the forward transport phase. This is probably because at this time the subject required maximum wrist dorsal flexion to grasp a glass that has some weight, which optimized the tenodesis effect and the ability to pick up an object. The elbow extension was greater in both tetraplegia groups and occurred in the back transport phase, perhaps also because elbow extension favored the tenodesis effect in the wrist (Figure 7).
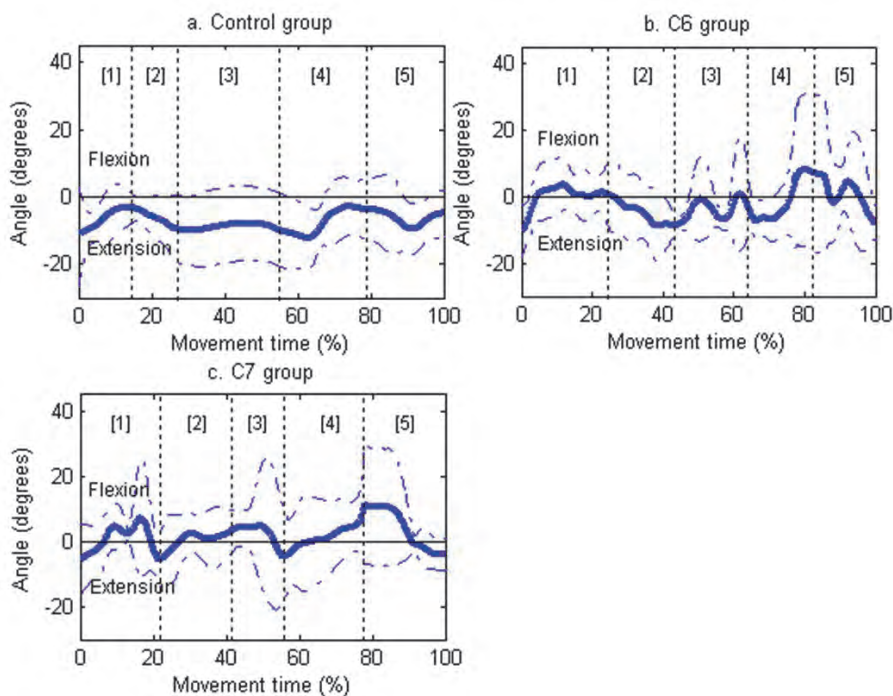
Fig. 7. Wrist dorsal-palmar flexion. Joint angles for wrist (dorsal flexion-downward, palmar flexion-upward). Figures 9a, 9b and 9c show the mean (continue thick line) and standard deviation (dashed line) of the CG, subjects with C6 tetraplegia and subjects with C7 tetraplegia, respectively. The vertical lines delimit the duration of the phases for each group. [1] reaching, [2] forward transport, [3] drinking, [4] back transport, and [5] return to beginning.

Mean retest values were within for the 95% confidence interval of the first test. Based on this data, it can be concluded that there were not differences between the test and retest with a probability of 95%. However, for measurements as maximum shoulder flexion, maximum external rotation, maximum elbow flexion, maximum pronation, even maximum wrist palmar flexion, wide confidence intervals were obtained. It could be probably due to the natural large variation between the subjects in those measurements. It is necessary to take into account that people can perform a goal-oriented task with many different combinations of individual joint movements.

2.3 Upper limb biomechanical model for virtual reality application
Human body movement is developed in a 4 dimensional space (3 spatial dimensions and time dimension). Each body segment takes orientations in the spatial space as long as movement is performed. This added to the well known articulated chain setup of the arm, causes that each segment takes several interrelated positions during movement, drawing their own trajectory in space in a complex manner. This complexity makes more difficult the comprehension of movement and the integration of movement information into clinical

application. Therefore, a new model of movement representation that facilitates its application is presented next and an application of this new biomechanical model as part of a virtual reality and motion capture rehabilitation system called TOYRA.

To reduce this complexity, movement is traditionally analysed in 2 dimensions, projecting or enclosing movement into an adequate plane. Positions and trajectories are drown in cartesian planes, referenced to the gravity centre of body and frequently orientations are described against anatomical planes (saggital, coronal and transverse planes) (Villalba 2003). This kind of representations are very appropriate to describe movements like human walking, that are almost always enclosed into one plane. Although they are not enough clean while trying to describe mentioned complex movements in space, most of the times due to the inconsistencies that those representations have.

In upper limb particular case, the references of the orientations and movements are defined at one arbitrary pose. Anatomic pose is very commonly used but not the only one. This pose consists in a body standing position, with the arm falling down resting and the hand palm looking to the front (Rau 2000). Motion-capture applications commonly use the t-pose. This pose consists in a body standing position, with the arm in lateral horizontal position, perpendicularly to body, and hand palm looking towards front or facing down.

Rodriguez et al (Rodriguez 2005) proposed to reference to anatomic pose with a small modification (hand palm in resting position towards the body) and tried to establish a comprehensive mathematical representation of 3D orientations for arm body segments. They opened the way of representing complex 3D movements of the upper limbs in a more precise & comprehensive manner (Rau, et al., 2002).

Present work identifies some inconvenient of those upper limb movement representations and completes Rodriguez et al formulation to a really univoque representation model. In first place, some simplifications will be described from the real human body model assumed in this work. After that, relevant clinical angles will be identified. Then, for each body segment former angle definitions (traditional and Rodriguez et al) will be analysed and new definitions will be proposed and discussed.

Then some simplifications from the real human body model are assumed to facilitate the analysis:

1. Each joint is defined through one articular centre, considered fixed to both joined segments. Specially, the shoulder joint, is considered as a simple spherical joint that follows same movement functionality of shoulders but not their real configuration.
2. The clavicle will be considered as part of thorax and its movements are not included (Ray and Schmidt, 2000).
3. The forearm is considered as a rigid body. Therefore pronation-supination movements must be reallocated in elbow joint.
4. The whole hand is modelled as one rigid-body. It will be considered as open hand.

Taking into account this simplifications, just seven elemental movements are required to describe the movement of upper limbs: three rotations on shoulder, flexo-extension of elbow, fore-arm rotation and two wrist rotations from fore-arm are considered to complete the description. These elemental movements are defined independently using planes and reference axis of the human body.

To analyse those 7 elemental movements, it is presented in next paragraphs a new definition proposal for poses & movements of upper limb based in previous proposals of Rodriguez et al and Rau et al., 2000. A vectorial model is used to measure and describe movements of

upper limb, formalizing the definitions of each of the mentioned elemental movements. To measure movements of one segment from previous segment of the chain is needed to define a local reference system for each segment. This reference system includes three unitarian and orthogonal vectors.
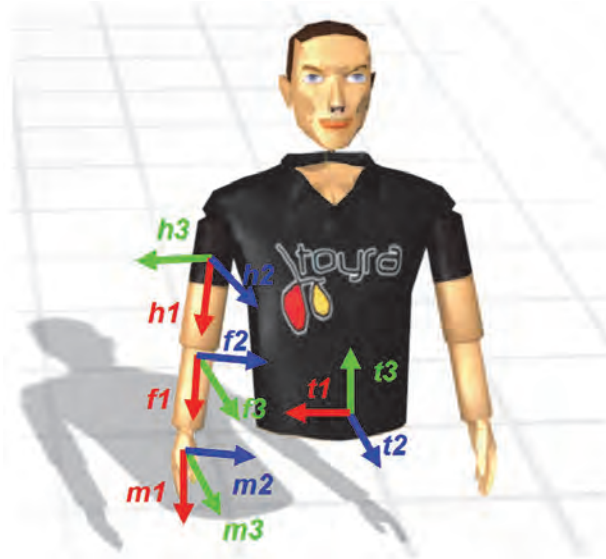

Fig. 8. Thorax, Humerus, Forearm and Hand reference system.

As global reference, it is defined a reference system fixed to the thorax (t1, t2, t3), as shown in Figure 8. Vector t1 follows transversal axis from one shoulder to another, vector t2 follows frontal axis from back to front of thorax and vector t3 follows vertical axis completing orthogonal base (t3 = t1 x t2). This reference system will be placed centred in the base of the thorax.

Local reference system of humerus movements **(h1, h2, h3)** may be defined as follows (Figure 8):

- Vector **h1** follows longitudinal axis of arm, fixed to humerus, from shoulder to elbow.
- Vector **h2** follows frontal axis (A) from back to front of thorax when arm rests vertically downwards.
- Vector **h3** follows transverse axis (T) from other shoulder to actual shoulder when arm rests vertically downwards, completing orthogonal base (**h3 = h1 x h2**).

This reference system will be placed in the centre of the shoulder joint. Then, Rodriguez et al. defined the humerus (or shoulder) movements as:

Humerus Flexion: represented by the angle formed between upper arm and coronal plane, it can be calculated as PI/2 radians less the angle formed between **h1** & **t2** vectors.

Humerus Abduction: represented by the angle formed between upper arm and saggital plane, it can be calculated as PI/2 les the angle formed between **h1** & **t1** vectors.

Humerus Rotation: is defined as the angular movement of humerus over its own longitudinal axis (over vector h1). To measure this angle is needed to move arm in a vertical downward just reducing flexion and abduction without longitudinal rotation. Therefore humerus will be aligned as **h1 = -t3** and rotation angle will be the angle formed by **h2** and **t2**.

They also established as reference for these movements (the anatomical pose): vertically downward extended arm without rotation. But these definitions do not establish a really univoque relation between arm positions and values of those three magnitudes (humerus flexion, abduction and rotation). To demonstrate this idea, we can analyze the elevation movement of the extended arm in the saggital plane for instance. According to Rodriguez definition, abduction will point to 0 radians all the time, and flexion will range from 0 to PI/2 (when arm gets perpendicular to the body) and again 0 radians (when arm gets upwards). Then zero values of flexion abduction angles may represent two different poses of the arm: vertically downwards or upwards. This also happens to every two symmetric positions of the arm to horizontal plane. It happens also in movements inside coronal plane with flexion = 0 and abduction varying from 0 to PI/2 and to 0 again. Another problem of Rodriguez's proposal is the lack of definition of humerus rotation angle. As long as reference system rotation is not a commutative operation, the humerus rotation angle result may vary as the alignment path is defined. For example, humerus rotation angle will be different if you first reduce humerus flexion or humerus abduction (as the first step to align **h1** and **t3** for instance). To avoid these problems, it is now proposed:

- To apply a differentiating criteria for angles below and over the transverse plane located at shoulder height. Humerus flexion when arm is located vertically downwards should value 0 radians, when arm is located horizontally perpendicular to body should value PI/2 radians and when is located vertically upwards should value PI radians. Same ranges for humerus abduction.

- To choose arbitrarily one path of alignment of **h1** and **t3** and always apply the same path. As long as many combinations may be established, the simpler one is selected: to rotate humerus through a single rotation to reach the alignment desired. Always it is possible to find appropriate rotation for any vector pairs, except when they are parallel. In this case, should be applied a symmetry transformation.

Therefore, humerus (or shoulder) movement definitions are reformulated as follows:

Humerus Flexion: represented by the angle formed between upper arm and coronal plane. It can be calculated as PI/2 radians less the angle formed between **h1** and **t2** vectors when **h1** is below transverse plane and as PI/2 plus the angle formed between **h1** and **t2** when **h1** is over transverse plane.

Humerus Abduction: represented by the angle formed between upper arm and saggital plane. It can be calculated as PI/2 less the angle formed between **h1** and **t1** vectors when **h1** is below transverse plane and as PI/2 plus the angle formed between **h1** and **t1** when **h1** is over transverse plane.

Humerus Rotation: is defined as the angular movement of humerus over its own longitudinal axis (over vector **h1**). To measure this angle is needed to rotate arm to a vertical downward pose just with one single rotation. Then humerus will be aligned as **h1 = -t3** and humerus rotation angle will be the angle formed by **h2** (rotated) and **t2**. If initial **h1** is parallel to **t3**, humerus rotation angle will be the angle formed by **–h2** and **t2**.

Applying this definitions, one pose is represented by only one combination of humerus flexion, abduction and rotation values and viceversa. It is established a really univoque relation. As it will be exposed in the examples included in next parragraphs.

Forearm movements are defined respect previous segment (the humerus), not from global reference system (Figure 10). It is defined a local reference system fixed to forearm (**f1**, **f2**, **f3**), following next considerations:

- Vector **f1** vector follows the longitudinal direction of the forearm from the elbow to the wrist.
- Vector **f3** vector is perpendicular to f1 and parallel to the wrist from ulna eminence to radius eminence.
- Vector **f2** completes the reference system to build a dextro-rotatory system.

Rodriguez et al defined then forearm movements as the humerus case referencing traditional concept to facilitate its comprehension:

Elbow Flexion: is the angle between **f1** and **h1** vectors plus PI/2.

Pronation-Supination: this movement occurs when the line formed by ulna eminence and radius eminence of the wrist rotate over forearm axis. In the arm model this would be considered as a rotation of forearm over its longitudinal axis not really possible. To measure this angle it is needed to align forearm and humerus in a way that **h1 = f1**. Then pronation-supination angle is formed between **h2** and **f3**.

And zero position of the forearm is defined respect to humerus position, when arm is completely extended (**h1** is parallel to **f1**) and hand palm looks toward leg. But again, as it happened for humerus, these definitions do not establish a really univoque relation between arm positions and values of elbow flexion and pronation-supination. Again there is a problem with the lack of definition of rotation angle, pronation-supination. Also the proposed forearm flexion origin does not fit with the proposed definition.

To avoid these problems, it is proposed:

- To reformulate flexion definition, eliminating constant term of PI/2.
- To arbitrary choose one path of alignment of **h2** and **f3**. Again to rotate forearm with a single rotation to reach the wanted alignment.

Therefore the forearm movement description is proposed as:

Elbow Flexion: is the angle between **f1** and **h1** vectors (according to zero position definition when arm is completely extended).

Pronation-Supination: is defined as the angular movement of forearm over its own longitudinal axis (over vector **f1**). To measure this angle is needed to extend arm completely. Then humerus will be aligned with forearm and **f1 = h1**. Then Pronation-Supination angle is formed by **h2** (once is rotated) and **f3**.

Applying this definitions, one pose is represented by only one combination of forearm flexion and rotation values and viceversa. As it will be exposed in next examples.

Last analyzed are hand movements. It is defined a local reference system fixed to hand (**m1, m2, m3**) describing its movements respect to forearm. In the proposed model hand is represented by only one rigid body. It will be considered that hand is open because this assumption will facilitate definition of vectors:

- Vector **m1** goes over hand palm from centre of wrist to the extreme of the fingers.
- Vector **m2** is perpendicular to hand palm.
- Vector **m3** is **m1 x m2**

Again Rodriguez et al defined then hand movements as before referencing traditional concept to facilitate its comprehension:

Radio-Ulnar deviation: it is the angle formed by vector **m1** and the plane that includes **f1 and f2** vectors. Then this angle can be measured as PI/2 less de angle between **m1** and **f3.**

Wrist flexion: it is the angle formed by vector **m1** and the plane that includes **f1 and f3** vectors. Then this angle can be measured as PI/2 less de angle between **m1** and **f2.**

Zero pose of the hand is defined when **m1** & **f1**, **m2** & **f2** and **m3** & **f3** are parallel.

These definitions have the same problems as the definitions of humerus flexion and abduction when angles are greater than PI/2, but as long as the hand cannot normally flex or deviate beyond that limit, the definitions by Rodríguez will be accepted without changes by now. As already mentioned, the proposed mathematical model is implemented in a new virtual reality and motion capture application for upper limb rehabilitation called TOYRA. It acquires segment orientations and reports clinical angle evolution to clinicians. TOYRA covers the whole process from patient assessment, therapy configuration and planning, treatment development and registration to exposition of relevant clinical information to physicians. Stroke, SCI or upper limb orthopedic pathology patients benefit from this system.

The main objectives for TOYRA system are:

- Increase patient motivation through inserting his rehabilitation activity in a virtual world and involving social interaction thanks to comparative performance scores table.
- Introduce objective information to facilitate proper assessment, treatment and supervision of patient's clinical process.
- Improve professional performance through offering objective information reports on patient evolution and configuring proper therapy plans and exercises for their patients.

The system was developed and validated by an integrated team with clinicians specialized in the field of SCI and engineers from top ITS company (National Hospital for Spinal Cord Injury at Toledo and Indra Sistemas S.A., Madrid, Spain). So far, 13 patients have been subjected to several interactive sessions with the system, in order to validate it and obtain enough information for building a normalized movement data base. The system has two fundamental parts: centralized therapy managing/information subsystem (TMIS) and interactive therapy subsystem (ITS) (Figure 9). The first subsystem is deployed in a network server and uses a relational data base to work. It exposes its functionality to users with a web application through the local area network. Every PC station on the network would have access to the application through a web browser. The second subsystem includes a wearable motion capture system and two graphical user interfaces in a specific PC work station (in the hospital version). It is possible to connect as much as work stations as wanted to the same server. The integration between both subsystems is built with web services. The server exposes the required operations that will be invoked by the work stations when needed.
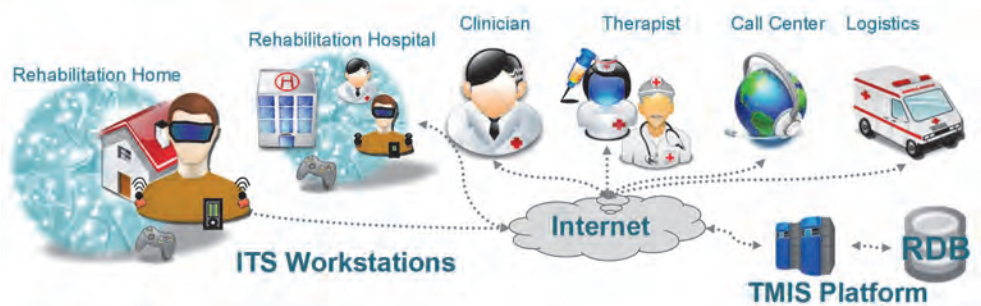

Fig. 9. TMIS and ITS subsystems.

From the functional perspective, the first subsystem includes the programming and planning of the patient's therapy, patient information managing, registry and access to the information

gathered from the second subsystem related to the therapy sessions, etc. From a functional point of view, the second subsystem has two orientations by user type - one on each graphical user interface. One of the user interfaces provides the information for the therapist to manage rehabilitation and interactive evaluation sessions. The other interface shows the patient for the patient a virtual reality environment with a specular avatar inside which mirrors the patient's every movement and displays visual cues for therapeutic exercises (as defined by clinicians).

Each subsystem has its own architecture scheme (Figure 10). The TMIS is based on Sun Microsystems Java 2 Enterprise Edition architecture, using Hibernate for persistent information, Apache Spring Framework for service layer construction, Adobe Flex for user web interface and Sun JAX-WS for web service interface. The ITS follows a very different architectural approach because it is a virtual reality system. It is developed in Microsoft C/C++ following the Indra's simulators architecture: several modules in form of Dynamic Libraries (DLLs) managed, coordinated and communicated through a host application developed under Windows platform. The modules covers every aspect from motion-capture to visualization, from calculations and information elaboration to reporting information to TMIS, from controlling therapy exercise logic to therapist graphical user interface.

TMIS SOA Architecture

	Client	Presentation	Business	Integration	Resources
Application	GUI Rendering Proxies DTOs	GUI Templates GUI Mediator Delegates DTOs	Interfaces POJOs	DAOs R/O Maps	Tables Directories Messages
Virtual Platform	Flash 9.0 DHTML + AJAX jQuery/Proto type	JEE5 Adobe Flex 2 JSF Framework	JEE5 Spring 2.5.0	JEE5 Hibernate JPA 3.2	SQL-92 LDAP v3 EAI w/HL7 2.x/3.x Legacy
Upper Platform	Internet Browser (1)	Web Server / Web Container JEE5 (2)	Application Server JEE5 (2)	Application Server JEE5 (2)	Backend Servers (Relational DBs, etc.) (2)
Lower Platform	User Operative Systems (1)	Server Operative Systems (2)			
Hardware Platform	User Hardware (1)	Server Hardware (2)			

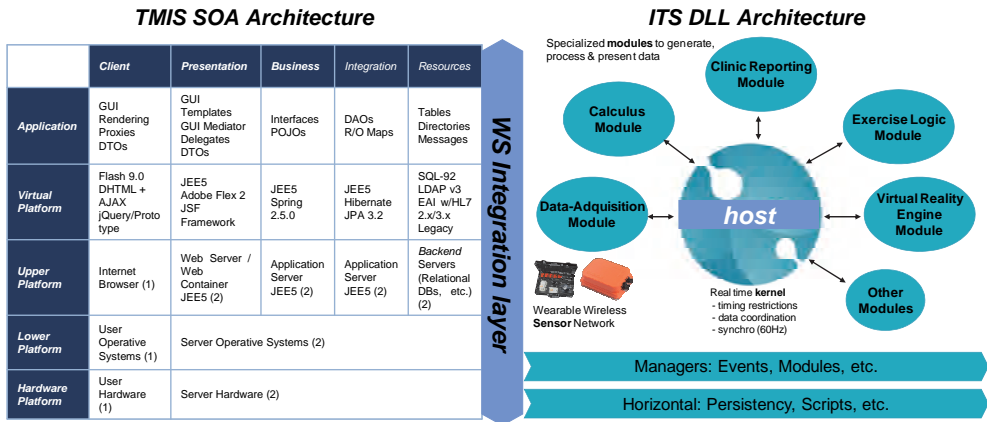*WS Integration layer*

ITS DLL Architecture

Fig. 10. TMIS and ITS architectures.

A very important component of the system is the motion capture sensors. After studying different solutions and technologies in this field, it was decided to use inertial sensors by Xsens Inc, an European manufacturer. Xsens has strong expertise in biomechanics and inertial sensor technology. The combination of expertise in human motion analysis and innovative inertial motion sensors makes Xsens a leader in inertial human motion capture solutions. There are several Xsens sensors models but in this case, the MTx model was the most appropriate for human motion capture as recommended by the manufacturer, and also because of their size and other features.

The MTx is a small and accurate 3DOF Orientation Tracker. It provides drift-free 3D orientation as well as kinematic data: 3D acceleration, 3D rate of turn and 3D earth-magnetic field. The MTx is an excellent measurement unit for orientation measurement of human body segments. The standard version MTx has a full scale acceleration of 5g, full scales of 18g are available as well. The MTx uses 3 rate gyroscopes to track rapidly changing

orientations in 3D and it measures the directions of gravity and magnetic north to provide a stable reference. The system's real-time algorithm fuses all sensor information to calculate accurate 3D orientation, with a highly dynamic response, which remains stable over time. Also an MT_X Development Kit is provided that allows users to take full advantage of the possibilities and the integration of the MTx with your own system. Pre-set user scenarios are available optimizing the Extended Kalman Filter routine for different applications. Based on the chosen scenario the MT_X will apply appropriate filter settings recommended for the application. The MTx is available as a stand-alone unit or as an Xbus version. On the Xbus (Xsens' digital data bus) multiple MTx's can easily be used simultaneously, enabling ambulatory and cost-effective measurement of human motion.

Then a DLL module was developed to capture body segment orientation in real-time. This data is captured from the sensor subsystem, through its driver which offers different formats for orientation data as rotation angles, quaternion, orientation matrix, etc. For this the orientation matrix format was chosen as it facilitates later calculations and avoids confusion about the order of arbitrary rotation angles.

Once the orientation data are available, another DLL module is responsible to insert it into a human body model, scaled to patient's anthropometric measurements (which are provided from TMIS). The avatar's movement as well as relevant clinical information are obtained from the human body model thanks to new algorithms developed specifically for this system (according to the model exposed in previous paragraphs). This clinical information includes flexion, abduction and rotation angles of each body segment, their maximums and minimums values, their velocities, etc. Therefore these algorithms convert from orientation matrix information from the body model to clinic angle information of each body segment under measurement. Then other DLL modules insert the avatar's movement into the virtual reality scenario and report relevant clinical information to TMIS through the web service interface. In Figure 11 examples are provided of virtual scenarios and avatars used for the system implementation.

In the near future the system scope will be extended to home care scenarios. It will also be validated with stroke patients as well as including more interactive virtual scenarios, emotional tagging and affective interface capabilities to increase patient motivation. Also sensor systems will be improved (miniaturization, wireless, cost, etc.) to make them more wearable and easily usable and accessibility and usability of the entire system will be revised. Finally based in the system described, some simple exercises will be showed below in order to demonstrate the proposed model coherence. For each exercise, description and angle graphs are provided. These graphs have in horizontal axis the percentage of movement (from start at 0% till end at 100%) and in vertical axis measured angle in radians.

Humerus frontal elevation – lateral descent: With humerus flexion and abduction fixed to zero, arm extended (vertically downward) and palm facing the leg, the patient raises their arm inside saggital plane until maximum angle is reached. Then the patient moves down their extended arm laterally (inside coronal plane). In the beginning of the downward movement, patient performs a humerus rotation until hand palm is facing outside to facilitate the descent. Movement is maintained until initial position (arm extended vertically downward) is reached (Figure 12). Humerus flexion, abduction and rotation are represented. Rest of measured angles are almost constantly zero except the of pronation-supination angle, which has a peak of approximately PI/2 over 55% of movement reasons why they will not be represented.

Fig. 11. Virtual scenarios and avatar´s used in the virtual reality environment. Evaluation exercises for patient assessment are performed in the bedroom scenario. Activities for daily living exercises are performed in the kitchen scenario. Wheelchair driving simulation takes place in the street (big open square). Other avatars used are also included.
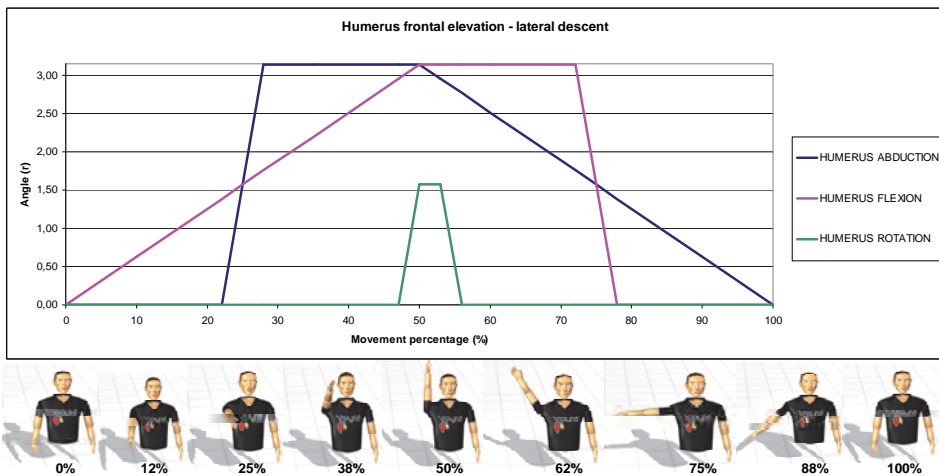

Fig. 12. Humerus frontal elevation – lateral descent

Note that the humerus abduction angle jumps from 0 to PI when the transverse plane is crossed on the way up (at 25% of the movement) while humerus flexion raises continuously. In the way down, humerus flexion angle jumps from PI to 0 when crossing transverse plane (at 75% of the movement) and humerus abduction angle descents continuously until 0 is reached. This is consequence of new definition and helps to differentiate when movement takes place in lower or upper spaces. This way coherence is achieved in the expected values of flexion and abduction angles at upwards pose. Also there is a peak in humerus rotation over the 50% of the movement because of the singularity of the upwards position of the arm.

Forearm elevation: With humerus flexion and abduction fixed to zero, arm extended (vertically downward) and palm facing the leg, patient elevates only the forearm inside saggital plane until maximum angle is reached. To help this movement, patient pronates allocating palm hand facing to shoulder in the last phase of movement. Elbow flexion, pronation and hand flexion are represented (Figure 13). Rest of measured angles are almost constantly zero figure 12.
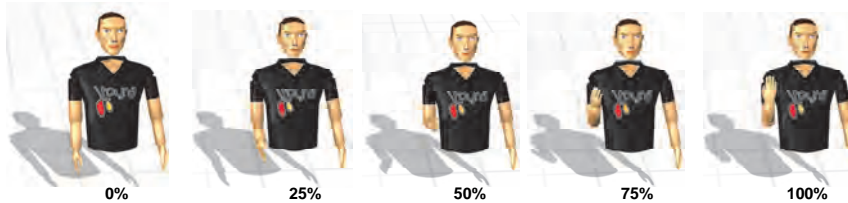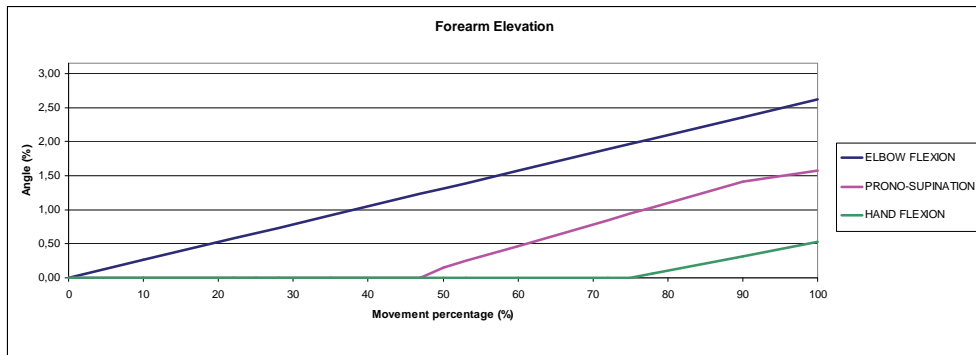

Fig. 13. Forearm elevation

Note that in this exercise elbow flexion raises from 0 to almost PI radians. In the second phase of the movement over transverse plane pronation-supination is performed to facilitate movement towards patient's shoulder. This angle raises from 0 to PI/2 radians. At the end of the movement, also wrist flexion increases a little bit to touch shoulder.

2.4 Estimation of upper-limb biomechanical characteristics based on gyroscopes

Part of the population with SCI presents upper limb involuntary movements, such as tremor, clonus or spasmodic movements (Jankovic and Van der Linden, 1988). There is an absence of studies in the literature centred in the analysis of the involuntary movement behaviour in each articulation of the upper limb. The majority is focused on the

measurement of movement at the distal part of the arm. The analysis of involuntary movements at joint level provides information of foremost importance in the design of robotic solutions for rehabilitation, for instance the selection of the appropriate actuator technology to be used by a powered upper limb exoskeleton. In addition, it provides key information to estimate the efforts and to define the exoskeleton structure, (Rocon et al, 2007). This section will introduce an estimation of tremor kinematic parameters by reproducing upper limb kinematics based on a biomechanical model. It will be particularly focused on the estimation of parameters related to tremorous movements but could be extended to other sort of involuntary movements. The method used for the analysis of tremorous movements is based on a combination of solid modelling techniques with anthropometric models of the upper limb, allowing to develop a kinematic and dynamic upper limb model. This model of upper limb musculoskeletal systems allows the estimation of the force contribution of each muscle component during motion, the experimentation of modifications of the musculoskeletal topology as well as the comprehension of complex motion coordination strategies. The input of the model is the angular position, velocity and acceleration of each joint measured by gyroscopes placed at the upper limb of patients suffering from tremor.

The complexity of the musculature together with the difficulty of using non-invasive investigation methods, prevents accurately identifying the function of each muscular component. This work presents the analysis for the development of theoretical kinematic and rigid-body models of the human upper limb, on the basis of former investigations on the upper limb anatomy and biomechanics. A biomechanical model of the upper limb has been built in order to describe its kinematics and dynamic. According to current literature, bones may be regarded as rigid bodies in contrast to soft tissues, with respect to the relevant physiological ranges of motion and force handling. This allows the isolation of the skeletal subsystem from the soft tissues by converting their relations with the bones into external actions. The upper limb kinematics and dynamics may then be analyzed and modelled in considering the skeletal components only, (Maurel, 1999). Neglecting the hand, the human upper limb may be described as composed of five bones, the clavicle, the scapula, the humerus, the ulna and the radius, forming two mechanisms, the shoulder and the elbow. Their association allows a wide range of combined motions, and confers to the human arm the highest mobility in the human body, (Kapandji, 1983). In our study we are only considering the following degrees of freedom: elbow flexion-extension, forearm pronation-supination, wrist abduction-adduction, and wrist flexion-extension, (Rocon et al., 2007).

The forearm movements have been proved to be independent from each other, Youm, et., 1997. Physiologically, no fixed axis or rotation centre can be recognized in a real joint. For most joints, the relative motion between bones is a combination of rolling and gliding with pressure on the contact areas. An accurate joint model should account for all these movements as well as the forces and torques induced on the bones. A 2-D theoretical analysis was lead in this direction by Engin in 1984. The model described the relative motion between two bones, including both geometrical and material nonlinearities as well as the ligament and contact, forces and torques, (Engin, 1984). Another approach towards joint dynamics simulation was presented by Chao et al. The technique, named Rigid Body Spring Model, consisted of modeling the articular surface pressure with distributed compressive springs. When subjected to tensile forces, the compressive springs were removed from the

model. An iterative scheme was thus used to solve the system for the equilibrium, whereas the spring redundancy was handled by energy optimization. It was applied to static analysis of the wrist and hand biomechanics, (Chao et al., 1993). In most cases, however, translations appear negligible with respect to rotations, so that the model development and analysis may be simplified using idealized joints. In a 3-D space, an object may be characterized with respect to some reference coordinate system by 6 parameters: 3 related to the position and 3 related to the orientation of the segments. The mobility of a mechanism corresponds to its number of independent kinematic parameters, therefore called degrees of freedom (DOF). Considering these definitions, the skeleton mobility may be completely described by analyzing the joint kinematics. The general procedure is to individually consider the true functional mobility of each joint before considering the interdependencies induced by loops. In most analysis (Kapandji, 1983), the upper limb joints were idealized in the form of 3-DOF Ball & Socket 3-DOF Ball & Socket 2-DOF Hinge or 1-DOF Hinge rotational joints. Regarding dynamics, in most approaches, the upper limb has been assumed to be composed of rigid bodies, including the bones and the soft tissues attached to them, connected by ideal (frictionless) kinematic joints. The rigid bodies have been assumed to possess fixed centres of gravity, and the joints, fixed axes or centres of rotation, (Raikova, 1992).

Our approach has been build taking into account the Leva (de Leva 1996) and Zatsiorsky and Seluyanov tables (Zatsiorsky et al., 1990). These tables are the most widely accepted information within the field of biomechanics in order to perform dynamic analysis. In particular in sports and medical biomechanics. Leva adjustments has been made in order to define accurately the anthropometric measurements required to obtain inertial parameters from Zatsiorsky tables. A solid rigid model of the forearm has been build with the information taken from the above mentioned tables. The model has been parameterized using the Denavit-Hartenber approach. Finally a library has been made to allow a dynamical analysis of the system. This analysis has been done using the recursive algorithm from (Fu et al., 1987).

The model proposed consider the upper limb as a chain composed of three rigid bodies the arm, the forearm and the hand articulated on the rigid basis formed by the trunk and related by ideal rotational joints, (Maurel, 1999). This representation relies on three assumptions: 1) The mechanical behaviour of the upper limb with respect to the trunk is independent of the rest of the human body, 2) Each segment, bones and soft tissues have similar rigid body motions, 3) The deformation of the soft tissues does not significantly affect the mechanical properties of a segment as a whole. Assuming the hand motion has a negligible effect on the large motion dynamics of the upper limb, the hand was considered as a rigid extension of the forearm. Consequently, it has been necessary to determine a rigid body equivalent to the hand and forearm assembly to be substituted in the rigid body dynamic analysis. As a result, four rigid segments have been defined, in order to be able to analyse all the recorded degrees of freedom. Each segment is responsible for a degree of freedom: 1) Elbow flexion-extension, 2) Pronation-supination, 3) Wrist flexion-extension, and 4) Wrist deviation.

Two of these segments were virtual (No mass and no length). Each segment has attached its own Reference System (plus a coordinate frame for the all of them). In the Figure 14 can be seen the coordinate frames the defined and the degree of freedom represented per each system. The Denavit-Hartenberg parameters can be seen in table 1. For rotary elements, the parameter θ determines the position of the joint. That table then indicates the relationship

between the parameter and the physiological measured angle represented by β_i for each segment i. F_L means forearm length and H_L means hand length.
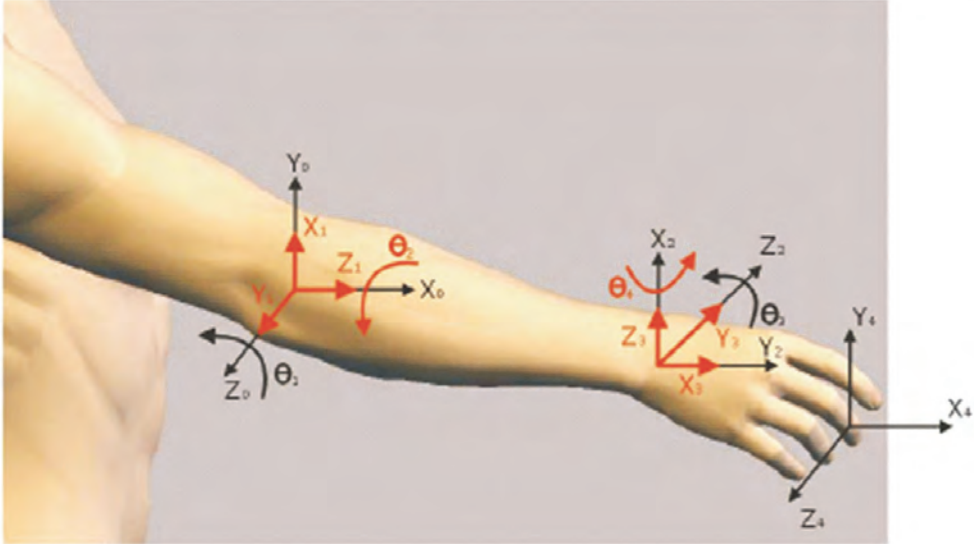

Fig. 14. Solid model representation of the forearm.

| Segment	d	a	θ	α
1 – Elbow F/E	0	0	$\beta_1 + \pi/2$	$\pi/2$
2 – Pronation	F_L	0	β_2	$\pi/2$
3 – Wrist F/E	0	0	$\beta_3 + \pi/2$	$\pi/2$
4 – Elbow Dev.	0	H_L	β_4	$\pi/2$

Table 1. DH parameters.

Biomechanical parameters per segment were obtained from previous report (de Leva, 1996). Segment 1 and Segment 3 are virtual; they are only defined to cope with the degrees of freedom of elbow flexion-extension and wrist flexion-extension respectively. However, when these segments are moved, the masses of the "real" segments are moved. All the inertial and mass parameters of a segment are defined below, using the following symbols: B_M, body mass, F_L, forearm length, F_M, forearm mass, H_L, hand length, H_M, hand mass, CoG_M, centre of gravity of each segment (obtained from Leva tables), and M_I inertia matrix. The computational algorithm used is based on the Newton-Euler equations of motion. Thanks to their recursive implementation, these equations of motion are the most efficient set of computational equations for running on a uniprocessor computer, so that implementation in real-time is possible.

$$M_1 = 0$$
$$CoG_1 = [0,0,0]$$
$$MI_1 = \begin{bmatrix} 0 & 0 & 0 \\ 0 & 0 & 0 \\ 0 & 0 & 0 \end{bmatrix}$$
$$M_2 = F_M = 1.6 \cdot \frac{B_M}{100}$$
$$CoG_2 = [0, F_L(0.457 - 1), 0]$$
$$MI_2 = \begin{bmatrix} 0.08 & 0 & 0 \\ 0 & 0.09 & 0 \\ 0 & 0 & 0.15 \end{bmatrix} \cdot F_M \cdot F_L^2$$

$$M_3 = 0$$
$$CoG_3 = [0,0,0]$$
$$MI_3 = \begin{bmatrix} 0 & 0 & 0 \\ 0 & 0 & 0 \\ 0 & 0 & 0 \end{bmatrix}$$
$$M_4 = = M_M = 0.6 \cdot \frac{B_M}{100}$$
$$CoG_4 = [0, H_L(0.79 - 1), 0]$$
$$MI_4 = \begin{bmatrix} 0.55 & 0 & 0 \\ 0 & 0.42 & 0 \\ 0 & 0 & 0.66 \end{bmatrix} \cdot H_M \cdot H_L^2$$

This analysis is intended to estimate the torque and power of the tremorous movement in each joint of the upper limb based on the information provided by the gyroscopes. Gyroscopes provide absolute angular velocity in its active axis, the combination of two independent gyroscopes, placed distal and proximally to the joint of interest, is required. Figure 15 illustrates the placement of the gyroscopes. With the gyroscopes in this position is possible to measure the following movements of the upper limb: Elbow flexo-extension, Forearm prono-supination, Wrist flexo-extension, Wrist deviation. In order to assess tremor biomechanical characteristics we have studied its behaviour in 31 patients suffering from different pathologies of tremor. A set of 6 tasks were select to excite tremor movements during the measurement session.
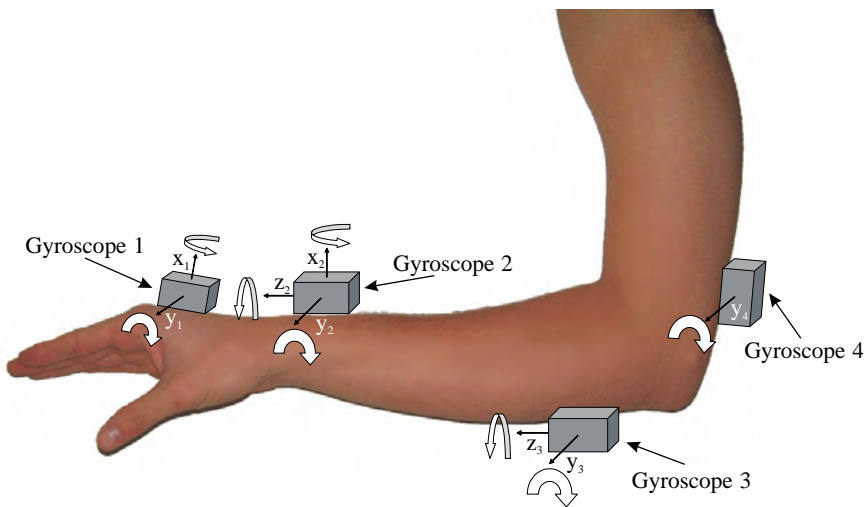
Gyroscope 1: Placed over the third metacarpal
Gyroscope 2: Placed over the edge of the forearm
Gyroscope 3: Placed bellow the olecranon process
Gyroscope 4: Placed over the olecranon process

Fig. 15. Gyroscopes placement.

Active orthoses are intended to counteract tremor by applying controlled forces. Torque is an essential parameter in the choice of the actuator technology that will be used by powered orthoses. Special care should be taken with this parameter since it presents a dynamic behaviour. As can be seen in Figure 16, this parameter presents a dynamic behaviour. The actuator technology that will drive the orthoses must be able to apply the same torque characteristics. Table 2 summarizes the mean value of torque estimated in each joint of the upper limb for the tasks of stretching out the arm and putting finger to nose. These tasks are shown because they are the ones in which maximum values of tremor activity were registered.
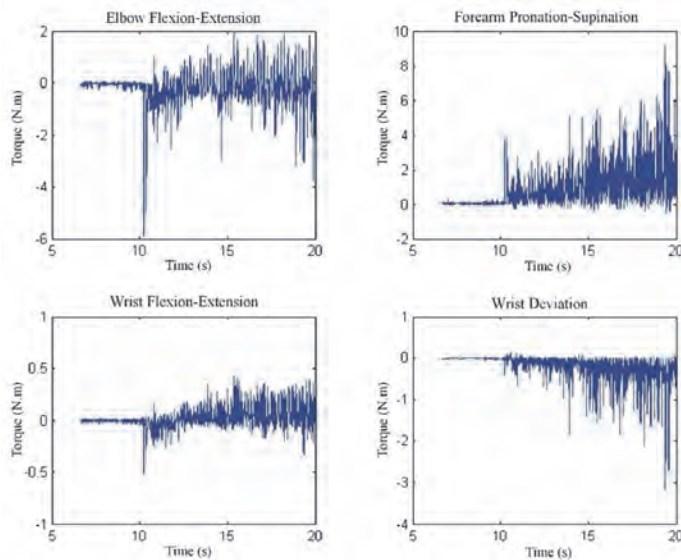

Fig. 16. Arm torques.

Movement	Finger to nose	Outstreched Arm
Elbow Flexo-extension	1.9 *N.m*	1.2 *N.m*
Forearm Prono-supination	3.7 *N.m*	1.9 *N.m*
Wrist Flexo-extension	0.4 *N.m*	0.2 *N.m*
Wrist Deviation	1.1 *N.m*	0.5*N.m*

Table 2. Mean values of the torque estimated in finger to nose and outstretched arm tasks

Movement	Finger to nose	Outstreched Arm
Elbow Flexo-extension	0.2 *W*	0.01 *W*
Forearm Prono-supination	1.8 *W*	0.2 *W*
Wrist Flexo-extension	0.08 *W*	0.03 *W*
Wrist Deviation	0.4 *W*	0.04 *W*

Table 3. RMS values of the power estimated in each joint during execution of finger to nose and outstretched arm tasks

The other important parameter is the power that the device can absorb. The amount of power consumed in relation to tremor is one of the key parameters that need to be taken into account in the design of these devices. The power at the joint plus the performance of the devices will also determine the battery capacity. Tremor is assumed to be a stationary movement and, leaving aside the viscous coefficient of joint braking, there is no effective work done on the joint. That is why the RMS value of the power estimated for the tremorous movement during the putting finger to nose and stretching out arm tasks are presented in Table 3.

The results of this study show the basis of the dynamics of tremorous movement in each joint of the upper limb, information that is required for the design of portable active upper limb exoskeletons. The model presented could be extended to the study of the biomechanical parameters of any other voluntary/involuntary movements associated to SCI patients.

3. Conclusion

Biomechanical analysis systems have turned out to be a powerful tool for a quantitative assessment of movement in all degrees of freedom. Up to now, upper limb biomechanical analysis is not so often presented in the literature and in clinical practice The variety, complexity and range of upper limb movements is a challenge to assessment and interpretation of data and the clinical routines for 3-D analysis in upper limbs are not fully established. There have been presented 4 different clinical applications of developing an upper limb biomechanical model. Clinical daily practice, robotics and virtual reality can be topics to apply upper limb biomechanical models.

4. Acknowledgment

5. References

Arai, T. & Kragic, D. (1999). Variability of Wind and Wind Power, In: Wind Power, S.M. Muyeen, (Ed.), 289-321, Scyio, ISBN 978-953-7619-81-7, Vukovar, Croatia

Bednarczyk JH, Sanderson DJ. (1994). Kinematics of wheelchair propulsion in adults and children with spinal cord injury. *Archives of Physical Medicine and Rehabilitation* 75: 1327-1334.

Biryukova EV, Roby-Brami A, Frolov AA, Mokhtari M. (2000) Kinematics of human arm reconstructed from spatial tracking system recordings. J*ournal of Biomechanics* 33:985-995.

Boninger ML, Cooper RA, Robertson RN, Shimada SD. (1997). Three-dimensional pushrim forces during two speeds of wheelchair propulsion. *American Journal of Physical Medicine and Rehabilitation* 76:420-426.

Boninger ML, Cooper RA, Baldwin MA, Shimada SD, Koontz AL. (1999). Wheelchair pushrim kinetics: body weight and median nerve conduction. *Archives of Physical Medicine and Rehabilitation* 80:910-915.

Brauer RL, Hertig BA. (1981). Torque generation on wheelchair handrims. *American Society Mechanical Engineering* AMD 43:113-116.

Broeks JG, Lankhorst GJ, Rumping K, Prevo AJ (1999). The long-term outcome of arm function after stroke: results of a follow-up study. *Disability and Rehabililitation* 21(8):357-364.

Chao E, Lynch J, and Vanderploeg M (1993) Simulation and animation of musculoskeletal joint systems. *Journal of Biomechanical Engineering*, 115: 562 – 568.

Cirstea MC, Levin MF. Compensatory strategies for reaching in stroke (2000). *Brain*, 123 (Pt 5): 940-953.

Clauser CE, McConville JT, Young JW. (1969). Weight, volume and center of mass of segments of the human body. AMRL-TR-69-70. Wright-Patterson Air Force Base, Yellow Springs (OH).

Collinger JL, Boninger ML, Koontz AM, Price R, Sisto SA, Toledrico ML, Cooper RA. (2008). Shoulder biomechanics during the push phase of wheelchair propulsion: a multisite study of persons with paraplegia. *Archives of Physical Medicine and Rehabilitation* 89: 667-676.

Cooper RA. (1995). Biomechanics of mobility and manipulation. En: Cooper RA editor. *Rehabilitation Engineering: applied to mobility and manipulation.* Medical Sciences Series. Bristol: Institute of Physics Publishing. p. 69-144.

Cooper RA, Robertson RN, VanSickle, Boninger ML, Shimada SD. (1996). Projection of the point of force application onto the palmar plane of the hand during wheelchair propulsion. *IEEE Transaction on Neural Systems and Rehabilitation Engineering* 4: 133-142.

Cooper RA, Robertson RN, VanSickle DP, Bonninger ML, Shimada SD. (1997). Methods for determining three-dimensional wheelchair pushrim forces and moments-a technical note. *Journal of Rehabilitation Research and Development* 34 (2):435-446.

Cooper JE, Shweddyk E, Quandbury AO, Miller J, Hildebrand D (1993). Elbow joint restriction: effect on functional upper limb motion during performance of three feeding activities. *Archives of Physical Medicine and Rehabiitation* 74:805-809.

Cooper R, Boninger M, Shimada S, Lawrence B. (1999). Glenohumeral joint kinematics and kinetics for three coordinate system representation during wheelchair propulsion. *American Journal of Physical Medicine and Rehabiitation* 78:435-446.

Curtis KA, Drysdale GA, Lanza RD, Kolber M, Vitolo RS, West R. (1999). Shoulder pain in wheelchair users with tetraplegia and paraplegia. *Archives of Physical Medicine and Rehabilitation* 76:360-367.

Dallmeijer AJ, Kappe YJ, Veeger DH, Janssen TW, van der Woude LH. (1994). Anaerobic power output and propulsion technique in spinal cord injures subjects during wheelchair ergometry. *Journal of Rehabilitation Research and Development* 31: 120-128.

Dallmeijer AJ, van der Woude LHV, Veeger HEJ, Hollander AP. (1998). Effectiviness of force application in manual wheelchair propulsion in persons with spinal cord injuries. *American Journal of Physical Medicine and Rehabilitation* 77:213-221.

De Leva P, Adjustments to Zatsioorsky-Seluyanov's segment inertia parameters. (1996). *Journal of Biomechanics*. 29(9): 1223 – 1230.

De los Reyes-Guzmán A, Gil-Agudo A, Peñasco-Martín B, Solís-Mozo M, del Ama-Espinosa A, Pérez-Rizo E (2010). Kinematic analysis of the daily activity of drinking from a glass in a population with cervical spinal cord injury. *Journal of NeuroEngineering and Rehabilitation* ,7:41.

Digiovine CP, Cooper RA, Boninger ML. (2001). Dynamic calibration of a wheelchair dynamometer. *Journal of Rehabilitation Research and Development* 38 (1): 41-55.

Dwan LN, McIntosh AS. (2006). Kinematics of the upper limb: A reaching and placing task with resistance in children. *Gait and Posture* 24(S):S235-S238.

Engin A. (1984) On the theoretical modelling of human joints. *Mathematical Modelling in Science and Technology,* J. R. Avula, Ed. Pergamon Press, New York, pp. 560–565.

Finch E (2002) Physical rehabilitation outcome measures: a guide to enhanced clinical decision making. 2nd edition. Hamilton, Ontario, Decker; 2002:ix,292.

Finley M, Rasch E, Keyser R, Rodgers M. (2004). The biomechanics of wheelchair propulsion in individuals with and without upper-limb impairment. *Journal of Rehabilitation Research and Development* 41: 395-402.

Fitoussi F, Diop A, Maurel N, Laassel EM, Pennecot GF (2006). Kinematic analysis of the upper limb: a useful tool in children with cerebral palsy. *Journal of Pediatric Orthopedics* 15(4):247-256.

Fu KS, Gonzalez RC, Lee CSG (1987). *Robotics: Control, Sensing, Vision, and Intelligence.* McGraw-Hill Book Company.

Gellman H, Sie I, Waters RL. (1988). Late complications of the weight-bearing upper-extremity in the paraplegic patient. *Clinical Orthopedic and Related Research* 233: 132-135.

Gil-Agudo A, del Ama- Espinosa A, Pérez-Rizo E, Pérez-Nombela S, Crespo-Ruiz B (2010). Shoulder joint kinetics during wheelchair propulsion on a treadmill at two different speeds in spinal cord injury patients. *Spinal Cord* 48: 290-296.

Gil-Agudo A, Del Ama-Espinosa A, Pérez-Rizo E, Pérez-Nombela S, Rodríguez-Rodríguez LP (2010). Upper limb joint kinetics during manual wheelchair propulsion in patients with different levels of spinal cord injury. *Journal of Biomechanics* 43:2508-2515.

Hanavan EP (1966) A personalized mathematical model of the human body. *Journal of Spacecraft* 3:446-448

Jaennerod M (1984). The timing of natural prehension movements . *Journal of Motor Behaviour* 16:235-254.

Jankovic J, Van der Linden C (1988). Dystonia and tremor induced by peripheral trauma: predisposing factors. *Journal of neurology, neurosurgery, and psychiatry*. 51(12):1512-9.

Kapandji I (1983) The physiology of the joints: Upper limb. Churchill Livingstone, 1983.

Koontz AM, Cooper RA, Boninger ML, Souza AL, Fay BT. (2002). Shoulder kinematics and kinetics during two speeds of wheelchair propulsion. *Journal of Rehabilitation Research and Development* 39:635-650.

Kulig K, Rao SS, Mulroy SJ, Newsam CJ, Gronley JK, Bontrager EL, Perry J. (1998). Shoulder joint kinetics during the push phase of wheelchair propulsion. *Clinical Orthopedics* 354:132-143.

Kulig K, Newsam CJ, Mulroy SJ, Rao S, Gronley JK, Bontrager EL, Perry J. (2001).The effect of level spinal cord injury on shoulder joint kinetics during manual wheelchair propulsion. *Clinical Biomechanics (Bristol, Avon)* 16:744-751.

Laffont I, Briand E, Dizien O, Combeaud M, Bussel B, Revol M, Roby-Brami A (2000). Kinematics of prehension and pointing movements in C6 quadriplegic patients. *Spinal Cord* 38(6):354-362.

Levin MF (1996) Interjoint coordination during pointing movements is disrupted in spastic hemiparesis. *Brain*, 119(1):281-293.

Linden ML, van Valent L, Veeger HE, van der Woude LHV. (1996). The effect of wheelchair handrim tube diameter on propulsion efficiency and force application. *IEEE Transactions on Neural Systems and Rehabilitation Engineering* 4: 123-132.

Magermans DJ, Chadwick EKJ, Veeger HEJ, van der Helm FCT (2005). Requirements for upper extremity motions during activities of daily living. *Clinical Biomechanics (Bristol, Avon)* 20:591-599.

Maurel W (1999) 3D modeling of the human upper limb including the biomechanics of joints, muscles and soft tissues.. Ph.D. dissertation, Ecole Polytechnique Federale de Lausanne.

Maynard FM, Bracken MB, Creasey G (1997). International Standards for Neurological and Functional Classification of Spinal Cord Injury. American Spinal Injury Association. *Spinal Cord* 35:266-274.

McCrea PH, Eng JJ, Hodgson AJ (2002) Biomechanics of reaching: clinical implications for individuals with acquired brain injury. *Disability and Rehabilitation* 24(10):534-541.

Mercer JL, Boninger M, Koontz A, Ren D, Dyson-Hudson T, Cooper R. (2006). Shoulder joint kinetics and patology in manual wheelchair users. *Clinical Biomechanics* 21:781-789.

Michaelsen SM, Luta A, Roby-Brami A, Levin MF (2001). Effect of trunk restraint on the recovery of reaching movements in hemiparetic patients. *Stroke* 32(8):1875-1883.

Mosqueda T, James MA, Petuskey K, Bagley A, Abdala E, Rab G (2004). Kinematic assessment of the upper extremity in brachial plexus birth palsy. *Journal of Pediatric Orthopedics* 24(6):695-699.

Murgia A, Kyberd PJ, Chapell PH, Light CM (2004). Marker placement to describe the wrist movement during activities of daily living in cyclic tasks. Clinical Biomechanics (Bristol Avon), 19(4):248-254.

Murphy MA, Sunnerhagen KS, Johnels B, Willen C. (2006). Three-dimensional kinematic motion analysis of a daily activity drinking from a glass: a pilot study. *Journal of Neuroengineering and Rehabiitation*, 3:18.

Murray IA, Johnson GR (2004). A study of the external forces and moments at the shoulder and elbow while performing every day tasks. *Clinical Biomechanics (Bristol Avon)* 19(6):586-594.

Nakayama H, Jorgensen HS, Raaschou HO, Olsen TS (1994). Compensation in recovery of upper extremity function after stroke: the Copenhagen Stroke Study. *Archives of Physical Medicine and Rehabiitation* 75(8):852-857.

Newsam CJ, Mulroy SJ, Gronley JK, Bonstrager EL, Perry J. (1996). Temporal-spatial characteristics of wheelchair propulsion. Effects of level spinal cord injury, terrain and propulsion rate. *American Journal of Physical Medicine and Rehabilitation* 75: 292-299.

Newsam CJ, Rao SS, Mulroy SJ, Gronley JK, Bontrager EL, Perry J. (1999). Three dimensional upper extremity motion during manual wheelchair propulsion in men with different levels of spinal cord injury. *Gait and Posture* 19:223-232.

Niesing R, Eijskoot F, Kranse R, den Ouden AH, Storm J. (1990). Computer-controlled wheelchair ergometer. *Medicine and Biological Engineering and Computer* 28:329-338.

Parker VM, Wade DT, Langton Hewer R (1986). Loss of an arm function after stroke: measurement, frequency and recovery. *International Rehablitation Medicine* 8(2):69-73.

Petuskey K, Bagley A, Abdala E, James MA,, Rab G (2007). Upper extremity kinematics during functional activities: Three-dimensional studies in a normal pediatric population. *Gait and Posture* 25:573-579.

Praagman M, Stokdijk M, Veeger HEJ. Visser B. (2000). Predicting mechanical load of the glenohumeral joint using net joint moments. *Clinical Biomechanics (Bristol Avon)* 15: 315-321.

Rab G., Petuskey K., Bagley A. (2002). Determination of kinematics of the upper extremity. *Gait and Posture* 15;2:.113-119.

Raikova R (1992) A general approach for modelling and mathematical investigation of the human upper limb. 1992. *Journal of Biomechanics* 25:857 – 867.

Rau G., Disselhorst-Klug., Schmidt R. (2000). Movements biomechanics goes upwards: from the leg to the arm. *Journal of Biomechanics*, 33(10):1207-1216.

Roby-Brami A, Feydy A, Combeaud M, Biryukova EV, Bussel B, Levin MF (2003). Motor compensation and recovery for reaching in stroke patients. *Acta Neurological Scandinavian* 107(5):369-381.

Rocon E, Belda-Lois JM, Ruiz AF (2007). Design and validation of a rehabilitation robotic exoskeleton for tremor assessment and suppression. *IEEE Transactions on Neural Systems and Rehabilitation Engineering* 15(3):367-378.

Rodriguez C., Quintero H., Aschner H. (2005) Movimiento del brazo humano: de los tres planos a las tres dimensiones. Revista de ingeniería de Universidad de los Andes, Bogotá, Colombia, núm 22 (nov-2005), pp. 36-44.

Rodgers MM, Tummarakota S, Lieh J. (1998). Three-Dimensional dynamic analysis of wheelchair propulsion. *Journal of Applied Biomechanics* 14:80-92.

Rodgers MM, Keyser RE, Gardner ER, Rusell PJ, Gorman PH. (2000). Influence of trunk flexion on biomechanics of wheelchair propulsion. *Journal of Rehabilitation Research and Development* 37:283-295.

Rönnqvist L, Rösblad B (2007). Kinematic analysis of unimanual reaching and grasping movements in children with hemiplegic cerebral palsy. *Clinical Biomechanics (Bristol Avon)* 22:165-17.

Safaee-Rad R, Shwedyk E, Quanbury AO, Cooper JE (1990). Normal functional range of motion of upper limb joints during performance of three feeding activities. *Archives of Physical Medicine and Rehabilitation* 71(7): 505-509.

Samuelson K, Larsson H, Tropp H. (1989). Wheelchair ergometer with a device for isokinetic torque measurement. *Scandinavian Journal of Rehabilitation Medicine* 21:205-207.

Sie IH, Waters RL, Adkins RH, Gellman H, (1992). Upper extremity pain in the postrehabilitation spinal cord injury patient. *Archives of Physical Medicine and Rehabilitation* 73: 44-48.

Subbarao J, KlopSiegwart, R. (2001). Indirect Manipulation of a Sphere on a Flat Disk Using Force Information. International Journal of Advanced Robotic Systems, Vol.6, No.4, (December 2009), pp. 12-16, ISSN 1729-8806fstein J, Turpin R. (1995). Prevalence and impact of wrist and shoulder pain in patients with spinal cord injury. *Journal of Spinal Cord Medicine* 18:9-13.

Tupling SJ, Davis GM, Pierrynowski MR, Shephard RJ. (1986). Arm strength and impulse generation: Initiation of wheelchair movement by the physically disabled. *Ergonomics* 29: 303-311.

Van Anden CJ, Wolterbeek N, Doorenbosch AM, Veeger HEJ, Harlaar J (2008). Complete 3D Kinematics of upper extremity functional tasks. *Gait and Posture* 27:120-127.

Van der Helm FCT, Veeger HEJ. (1999). Shoulder modelling in rehabilitation: the power balance during wheelchair propulsion. En: van der Woude LHV, Hopman MTE, van Kemenade C, editors. *Biomedical aspects of manual wheelchair propulsion: state of the art II.* Amsterdam: IOS Press. p. 96-103.

Van der Woude LHV, De Groot G, Hollander AP, van Ingen Schenau GJ, Rozendal RH. (1986). Wheelchair ergonomics and physiology testing of prototypes. *Ergonomics* 29:1561-1573.

Van der Woude LHV, Veeger HEJ, Dallmeijer AJ, Janssen TWJ, Rozendaal LA. (2001). Biomechanics and physiology in active manual wheelchair propulsion. *Medicine Engineering Physics* 23:713-733.

Van Drongelen S, Van der Woude LHV, Janssen TW, Angenot E, Chadwick EK, Veeger DH. (2005). Mechanical load on the upper extremity during wheelchair activities. *Archives of Physical Medicine and Rehabilitation* 86: 1214-1220.

Veeger HEJ, Rozendaal LA, van der Helm FCT.(2002). Load on the shoulder on low intensity wheelchair propulsion. *Clinical Biomechanics (Bristol Avon)* 17:211-218

Villalba M. (2003). Protocolo de análisis de movimiento en los brazos para diagnóstico clínco. Proyecto de grado en Ingeniería Mecánica. Universidad de los Andes. Bogotá. Colombia.

Wyndaele M, Wyndaele JJ (2006) Incidence, prevalence and epidemiology of spinal cord injury: what learns a worldwide literature survey? *Spinal Cord* 44:523-529.

Veeger HEJ, Rozendaal LA, van der Helm FCT.(2002). Load on the shoulder on low intensity wheelchair propulsion. *Clinical Biomechanics (Bristol Avon)* 17:211-218

Wu G, van der Helm F, Veeger H.E.J., Makhsous M, Van Roy P, Anglin C, Nagels J, Karduna A, McQuade K, Wang X, Werner F, Bucholz B (2005). ISB recommendation on definitions of joint coordinate systems of varius joints for the reporting of human joint motion- Part II: shoulder, elbow, wrist and hand. *Journal of Biomechanics* 38:981-992.

Youm Y, Cryer R, Thambyrajah K, Flatt A, Sprague B. (1997) Biomechanical analysis of forearm pronation-supination and elbow flexion-extension. *Journal of Biomechanics* 12:245 – 255.

Zatsiorsky V, Seluyanov V, Chugunova L (1990) Methods of determining mass-inertial characteristics of human body segments. *Contemporary problems of biomechanic.*, G. Cherny and S. Regiror, Eds. CRC Press, 272 – 291.